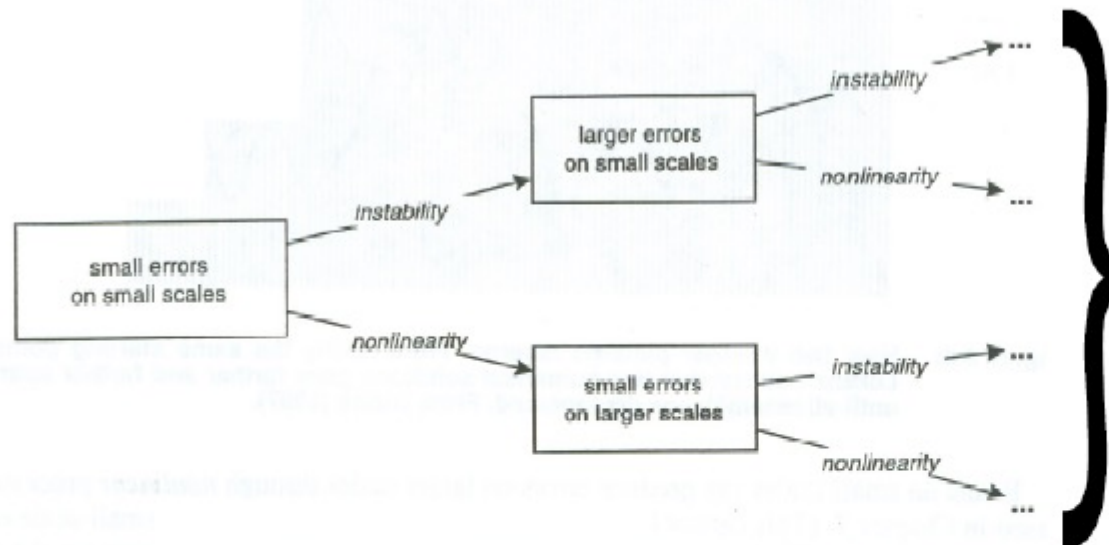


# 模式结果对初始条件的敏感性

## 上节课回顾

Instability (growth of small perturbations)  
Nonlinearity (interactions among scales)

Source: Dr. David Randall, CSU



Eventually, after time has passed, it is inevitable that even the very largest scales in a model will be dominated by great uncertainty.

Figure 8.9: Sketch illustrating the role of instability in leading to error growth, and of nonlinearity in leading to the movement of error from small scales to larger scales.

Any forecasting method is subject to this (not just numerical prediction) because the behavior of the system is heavily dependent on the initial conditions!

- there is a sensitive dependence on initial conditions

# 格距 .vs. 时间步长

## 模式参数设定

上节课回顾

$$\frac{\partial A}{\partial t} = -c \frac{\partial A}{\partial x}$$

Upstream scheme:

$$\frac{A(x, t + 1) - A(x, t)}{\Delta t} = -c \frac{A(x, t) - A(x - 1, t)}{\Delta x}$$

$$A(x, t + 1) = A(x, t) - c \frac{\Delta t}{\Delta x} [A(x, t) - A(x - 1, t)]$$

Courant Number  $c \frac{\Delta t}{\Delta x}$

Criteria of stability  $\left| c \frac{\Delta t}{\Delta x} \right| \leq 1$

## 上节课回顾

### Current trends in cloud models:

- Higher and higher resolution
- Studies include more simulations (no longer in the era of “one production run”)
- Ever increasing sophistication of microphysical parameterizations
- Increasing use of ensembles
- Increasing use of dynamical data assimilation techniques
- Operationally useful NWP that resolves smaller scale convective processes



北京大學

PEKING UNIVERSITY

# 强对流天气的可预报性



# 大气可预报性

- 指可以提前多长时间做出准确预报

$$\alpha(t) = \alpha(0) + t \times F$$

未来时刻 t 的大气

初始大气

影响大气变化的过程

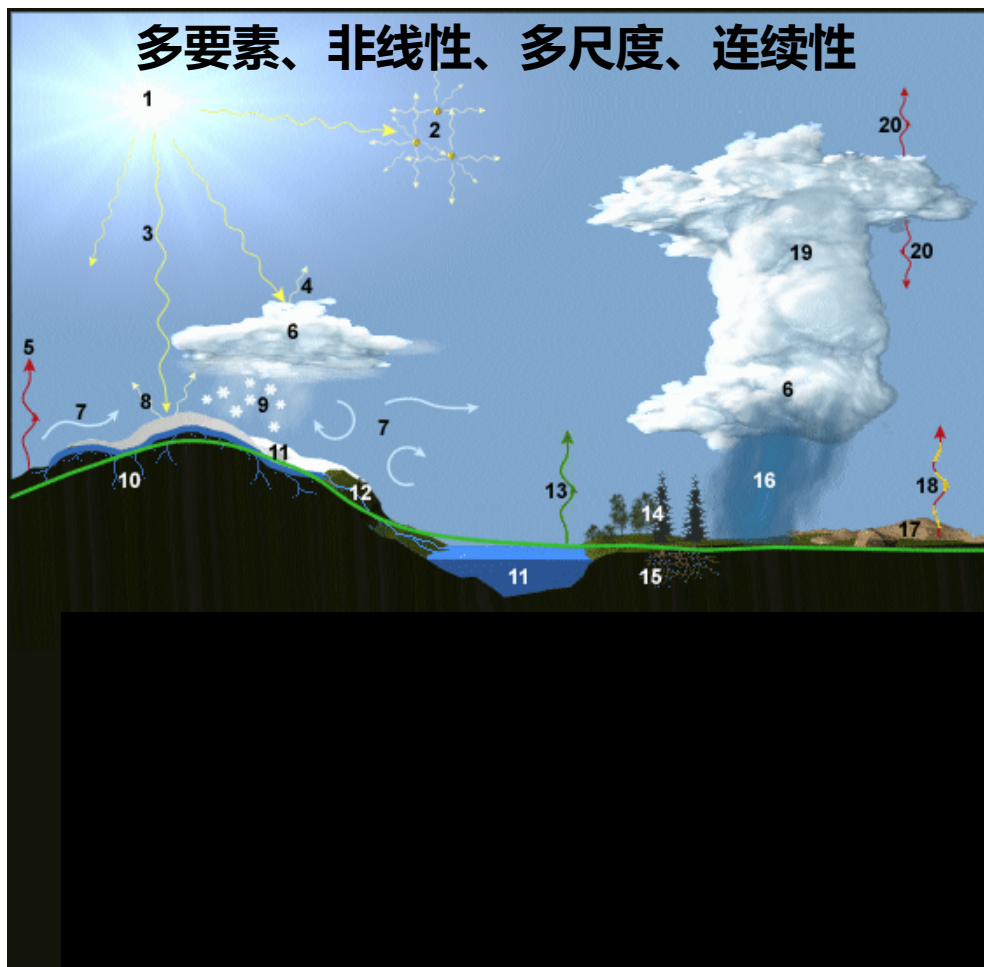
$$\frac{d\bar{u}}{dt} - f\bar{v} + \frac{1}{\rho_0} \frac{\partial \bar{p}}{\partial x} + \frac{\partial}{\partial z} (\overline{w'u'}) = 0$$

$$\frac{d\bar{v}}{dt} + f\bar{u} + \frac{1}{\rho_0} \frac{\partial \bar{p}}{\partial y} + \frac{\partial}{\partial z} (\overline{w'v'}) = 0$$

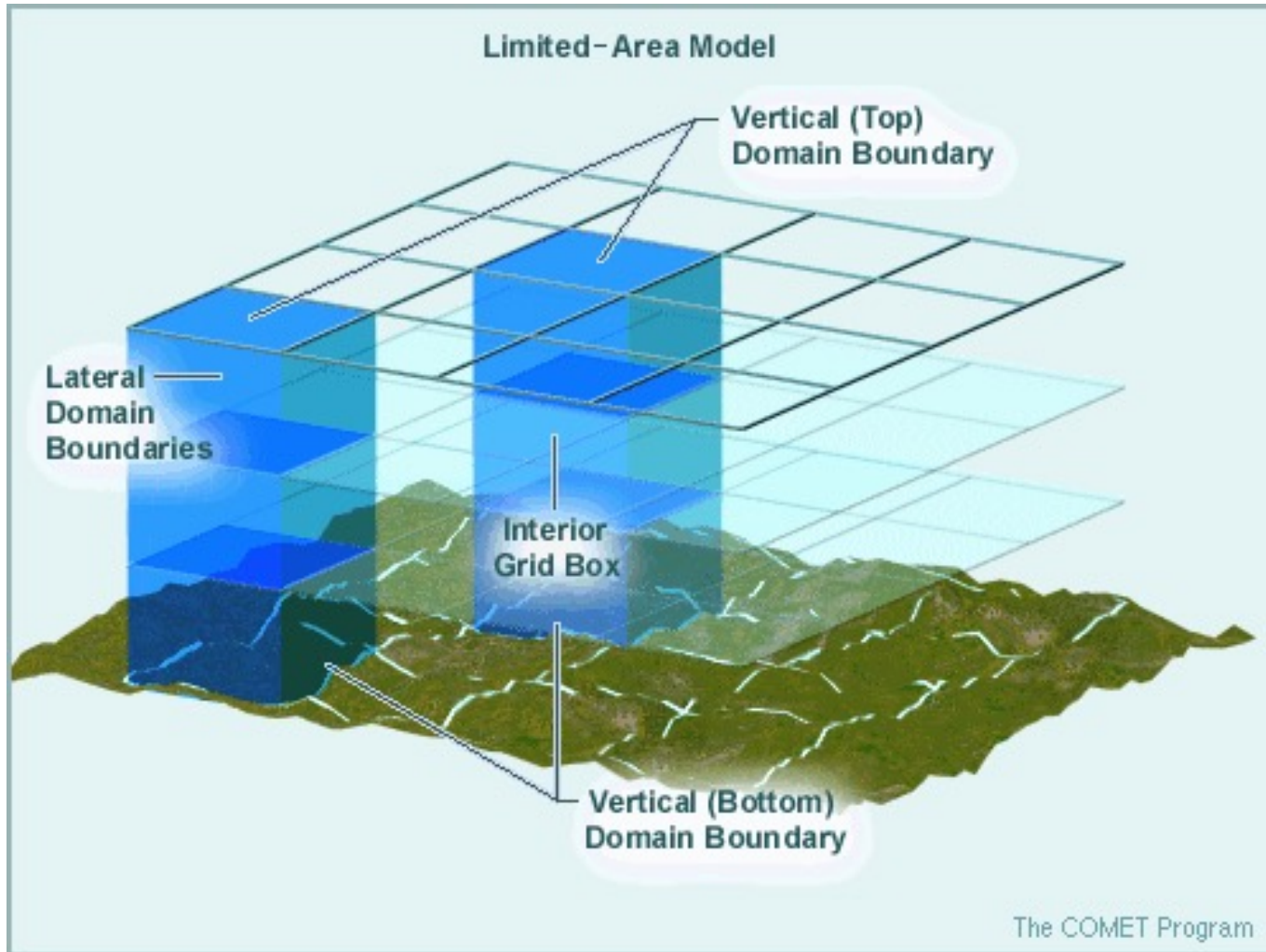
$$\frac{d\bar{\theta}}{dt} + \bar{w} \frac{d\theta_0}{dz} + \frac{\partial}{\partial z} (\overline{w'\theta'}) = 0$$

$$\frac{\partial \bar{p}}{\partial z} + g\rho_0 = 0$$

$$\frac{\partial \bar{u}}{\partial x} + \frac{\partial \bar{v}}{\partial y} + \frac{\partial \bar{w}}{\partial z} = 0$$

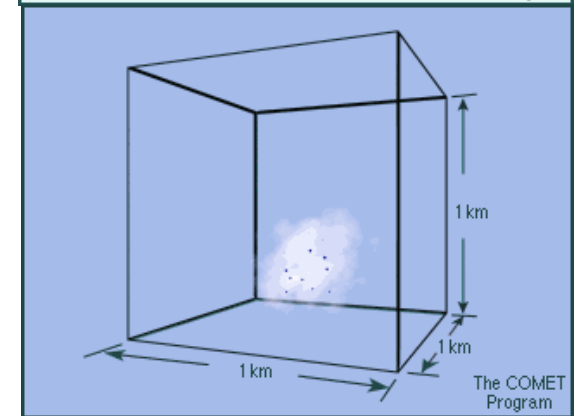
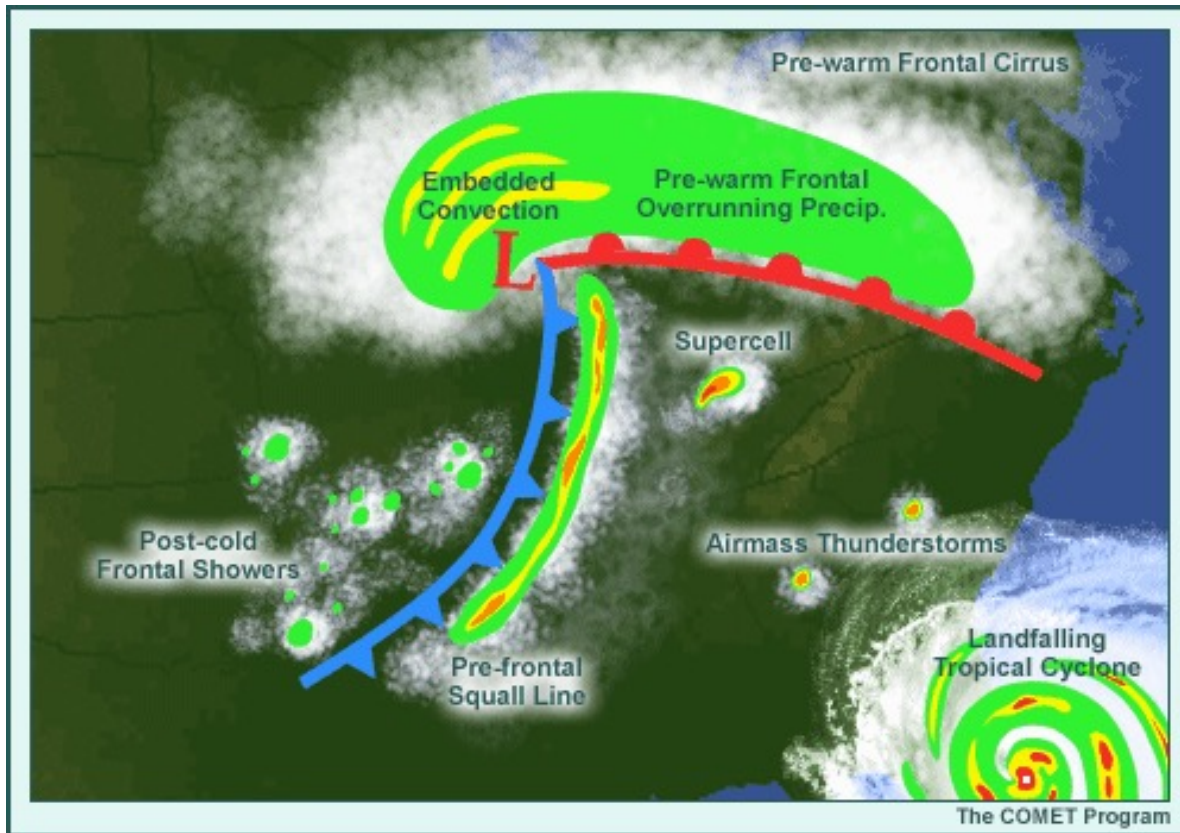


# 误差来源：离散化



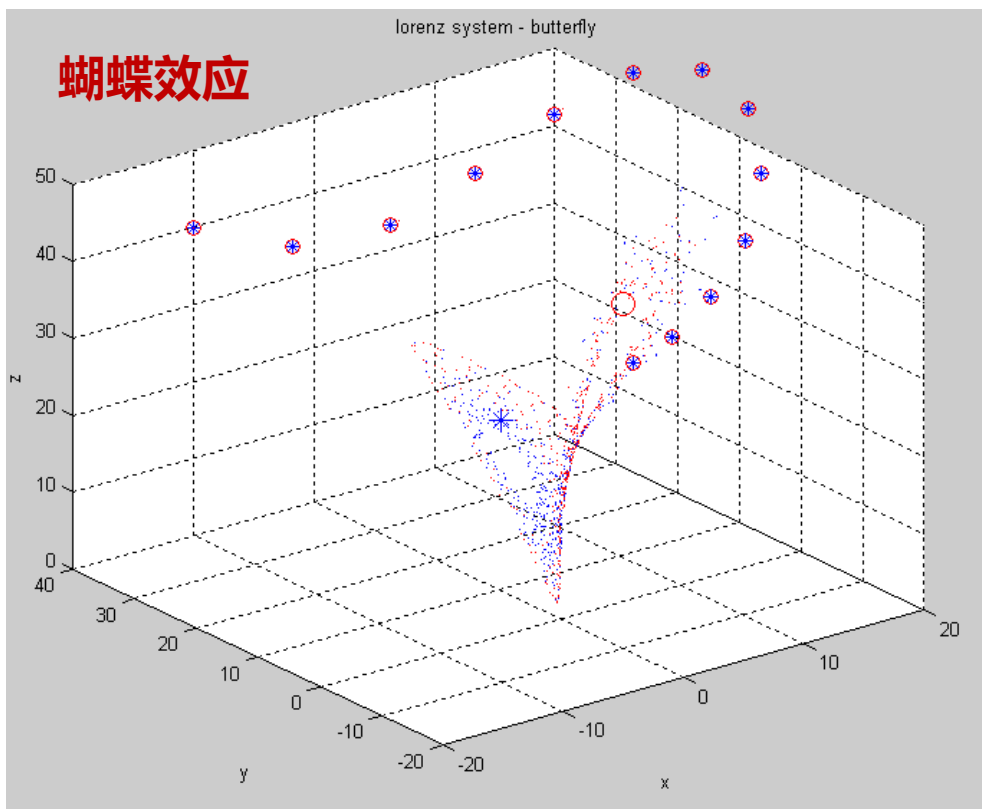
# 误差来源：初始和模式误差

- 观测时空密度和类别、资料同化算法
- 模式的物理过程描述

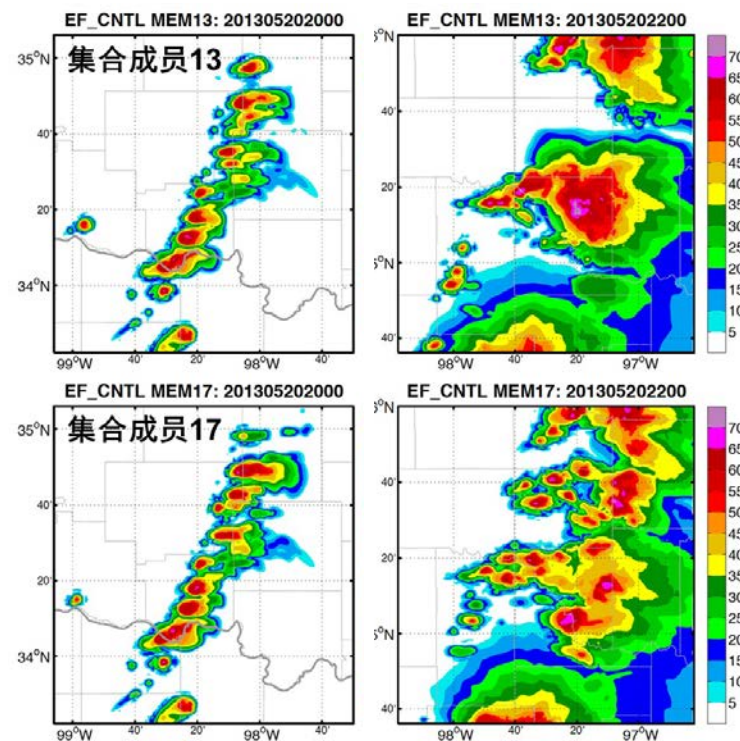


# 天气预报对误差的敏感性

- 初始很小的误差会造成一段时间后较大的误差
- 导致天气预报存在预报时效上限



## 2小时前后的雷暴预报差异



# 个例1：胞线

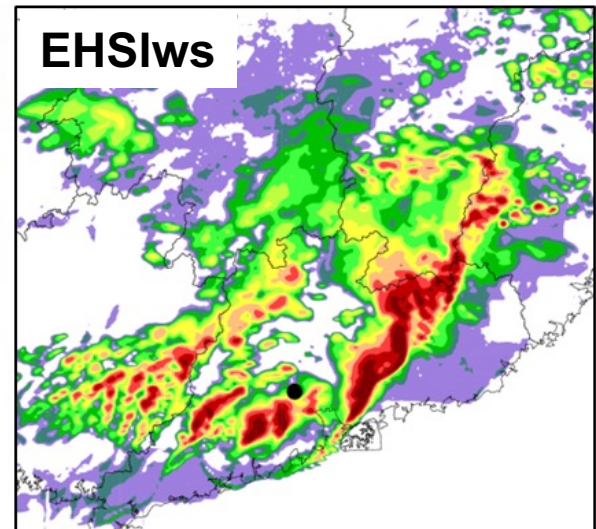
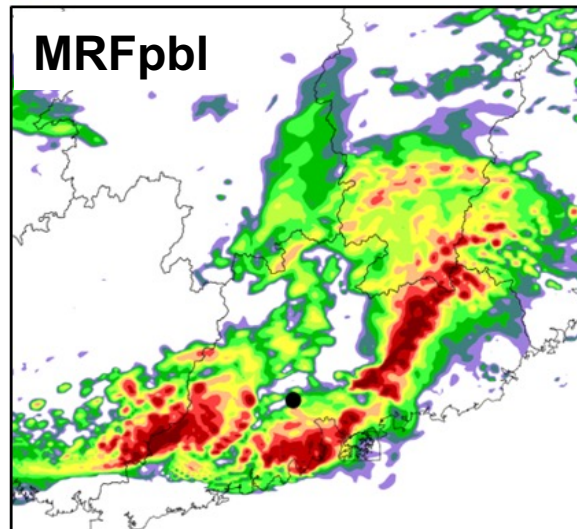
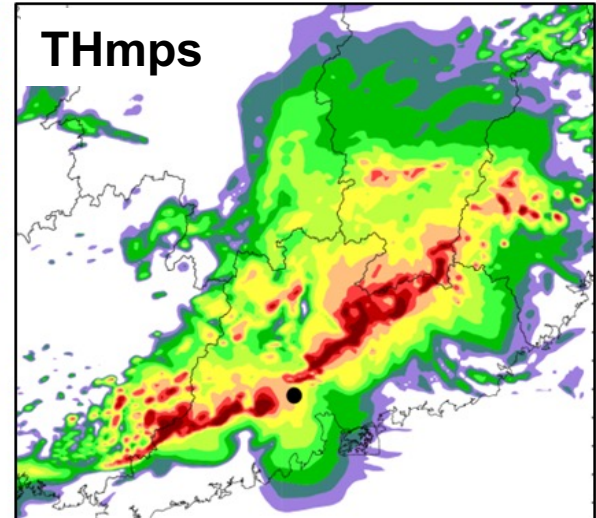
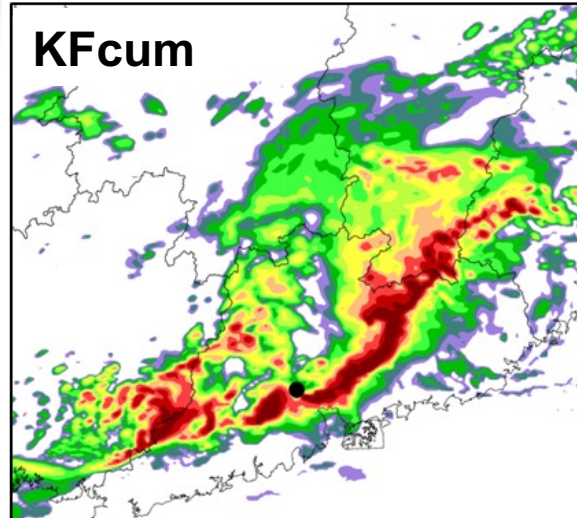
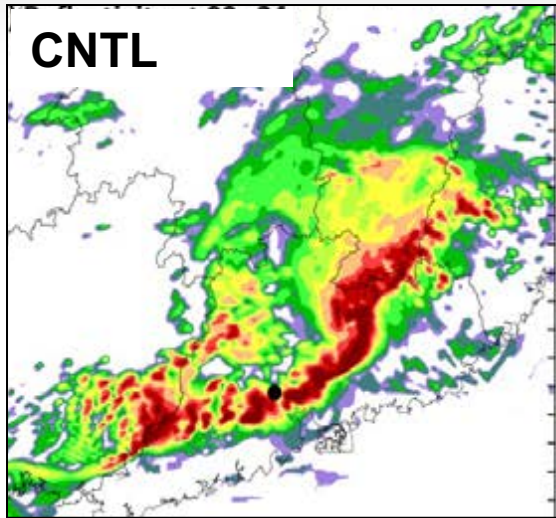
# The predictability of the squall line

(Wu, Meng, Yan , AAS, 2012)

- Sensitivity to the model error
  - Physical parameterization
  - Grid size
- Sensitivity to the initial error
- Possible way to improve the forecast skill



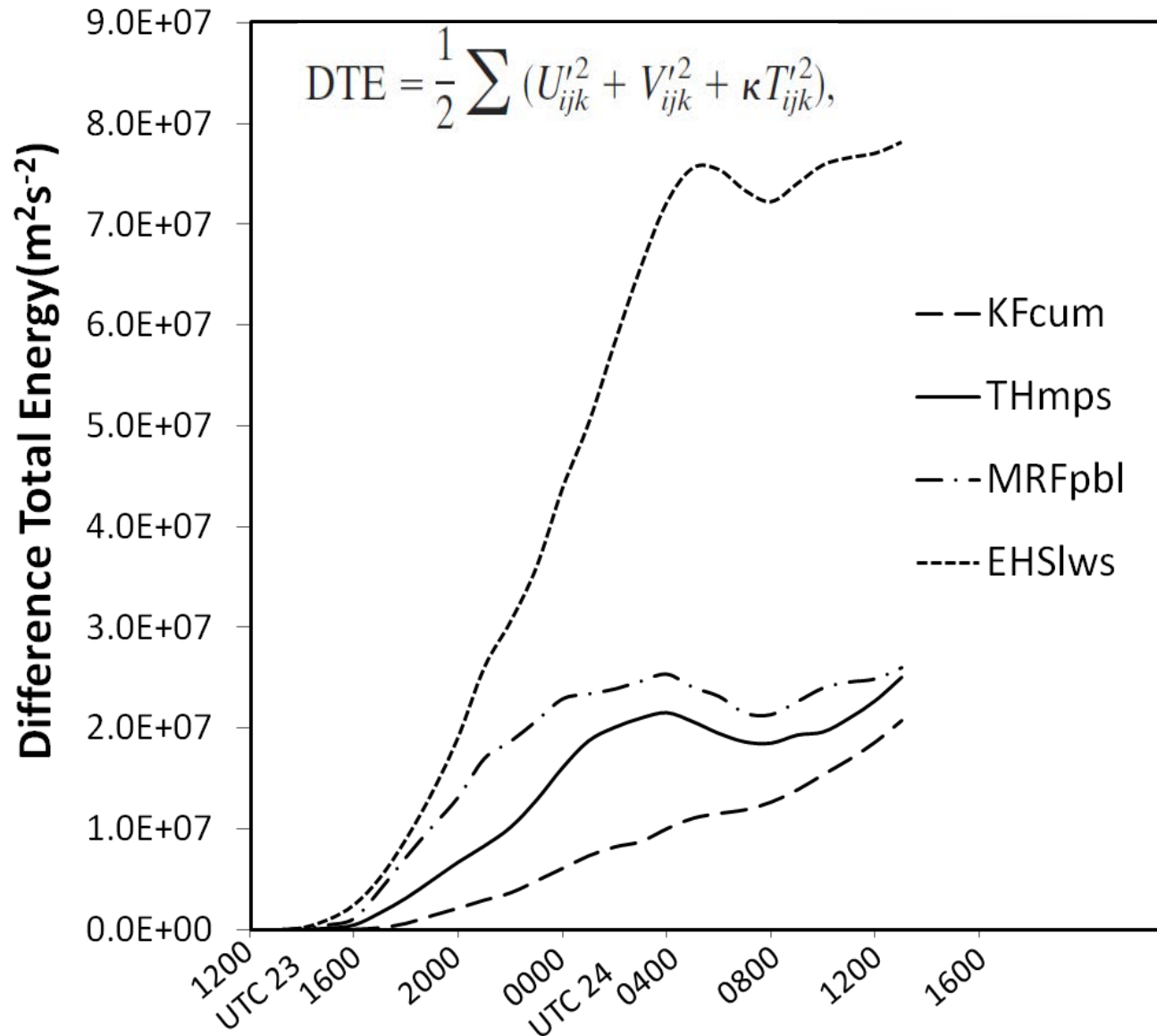
# Sensitivity to physical parameterization



**CNTL:** Grell  
WSM-6  
YSU  
NTM

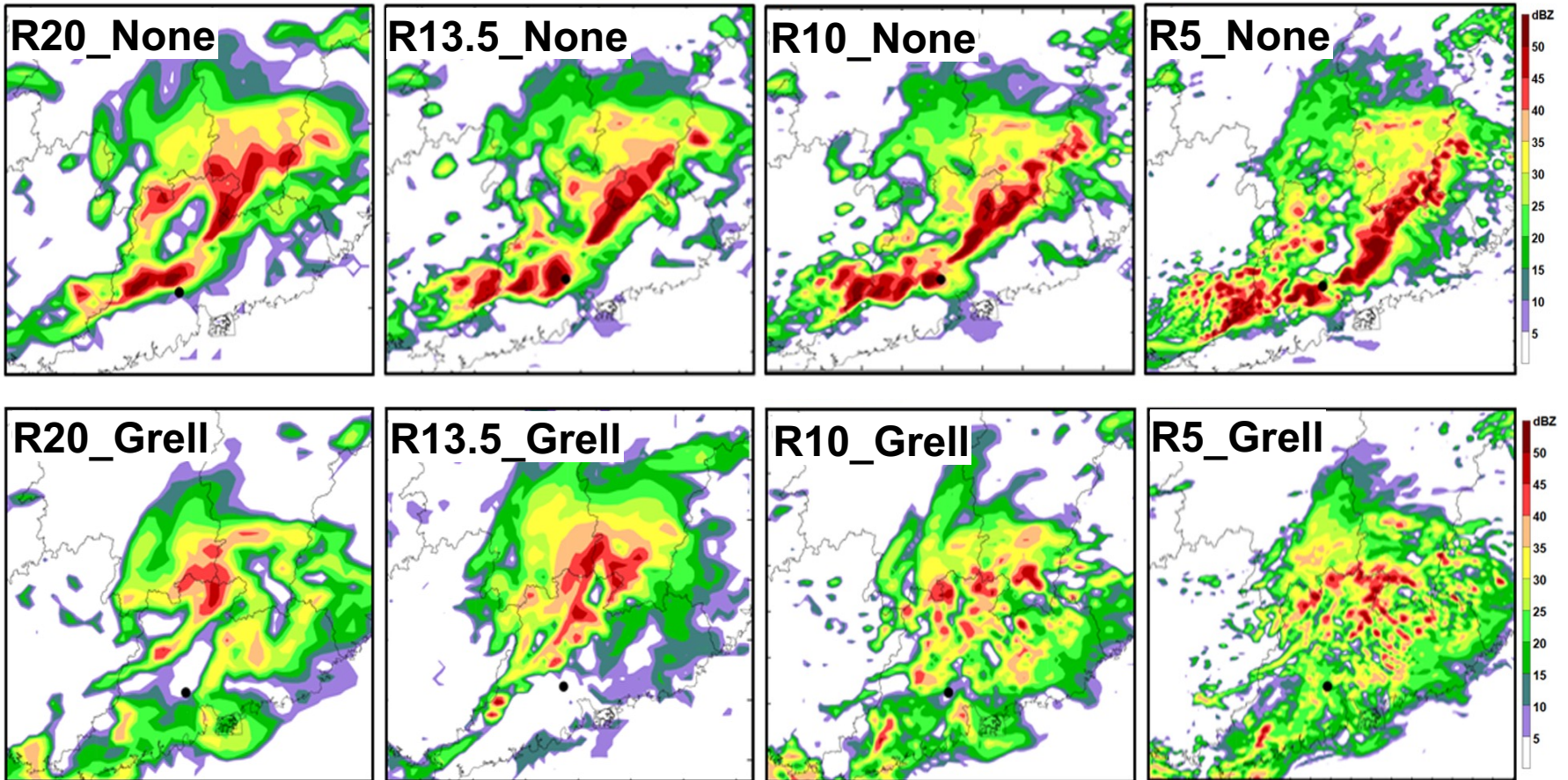
Expt.	Grid Size (km)	Cumulus schemes For D1 and D2	Microphysics schemes	PBL schemes	Longwave radiation schemes
C4.5	4.5	Grell-Devenyi for D1 & D2	WSM6	YSU	rrtm
KFcum	4.5	<b><i>Kain-Fritsch</i></b> for D1 & D2	WSM6	YSU	rrtm
THmps	4.5	Grell-Devenyi for D1 & D2	<b><i>Thompson</i></b>	YSU	rrtm
MRFpbl	4.5	Grell-Devenyi for D1 & D2	WSM6	<b><i>MRF</i></b>	rrtm
EHSlws	4.5	Grell-Devenyi for D1 & D2	WSM6	YSU	<b><i>EHS forcing</i></b>

# Impact of physical parameterization





# Sensitivity to grid size



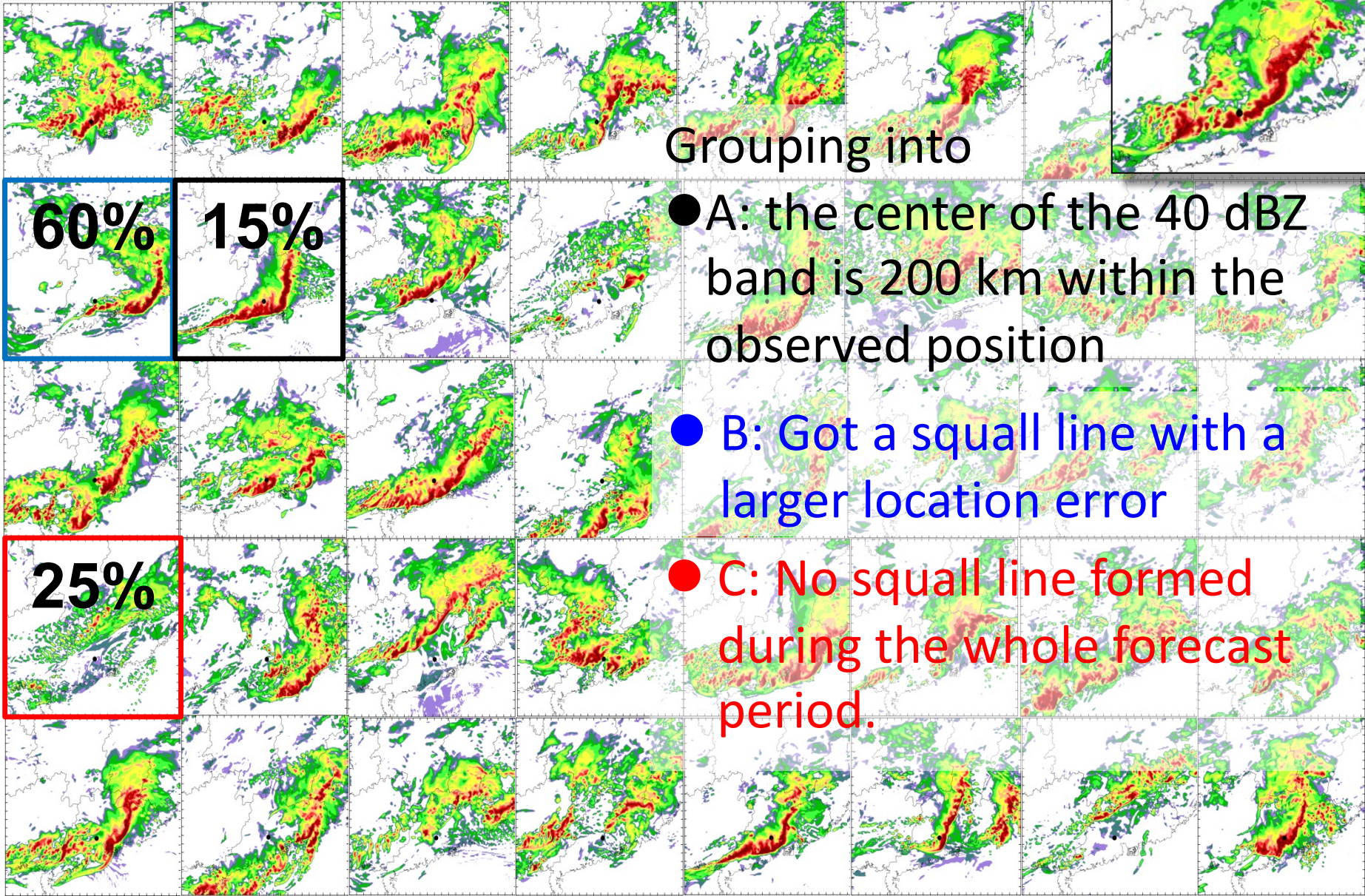
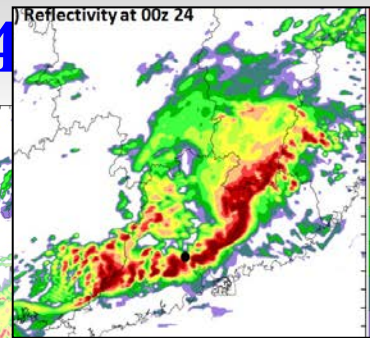
# Sensitivity to initial error

## Setup of ensemble forecast

- Initial ensemble : WRF-3DVar
- Ensemble size: 40
- STD: 1K for T, 2m/s for u and v, 0.5g/kg for qv



# The CNTL ensemble, reflectivity valid at 24



60%

15%

25%

Grouping into

- A: the center of the 40 dBZ band is 200 km within the observed position
- B: Got a squall line with a larger location error
- C: No squall line formed during the whole forecast period.

# Splitting experiments

$$\Delta = \{\text{initial}_{\text{good}} - \text{initial}_{\text{bad}}\} / 10$$

$$\text{All\_1} = \text{initial}_{\text{bad}} + \Delta * 1$$

$$\text{All\_2} = \text{initial}_{\text{bad}} + \Delta * 2$$

⋮

⋮

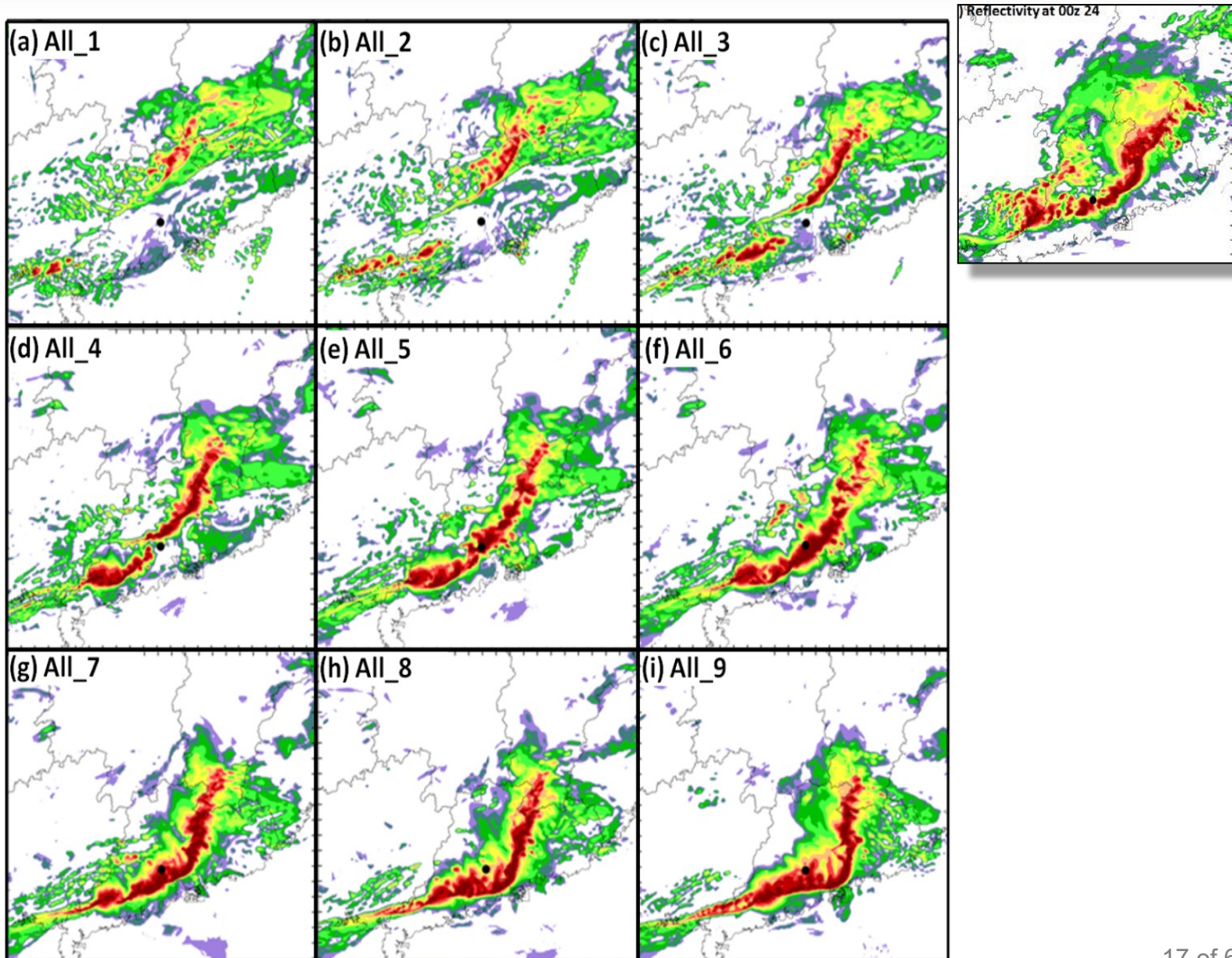
⋮

$$\text{All\_9} = \text{initial}_{\text{bad}} + \Delta * 9$$

(Melhauser & Zhang 2012)

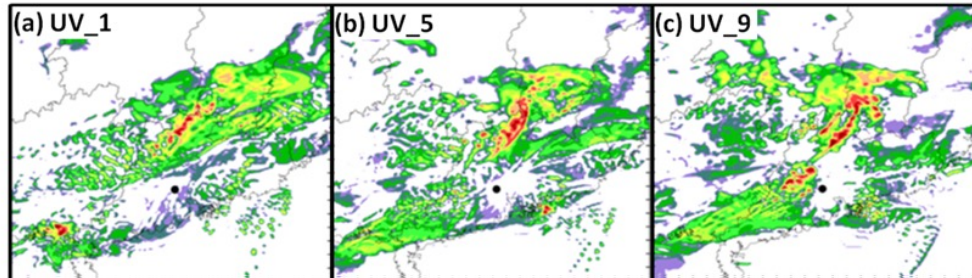


# Sensitivity to the initial error: all variables

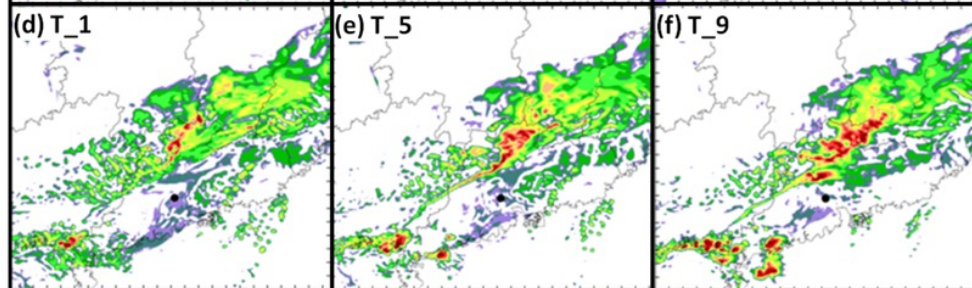


# Sensitivity to the initial error: different variables

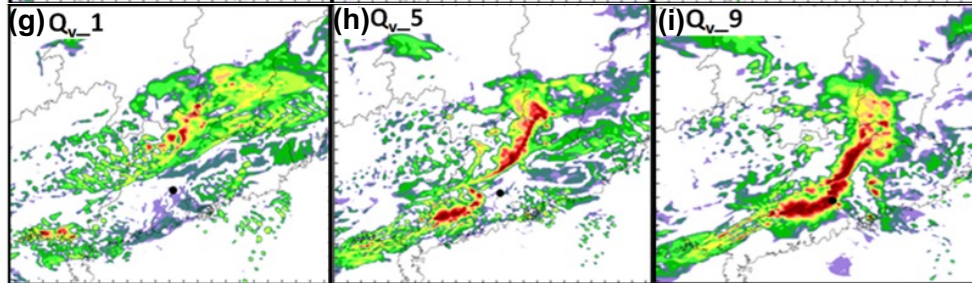
Only UV



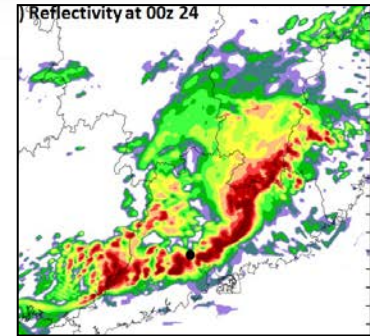
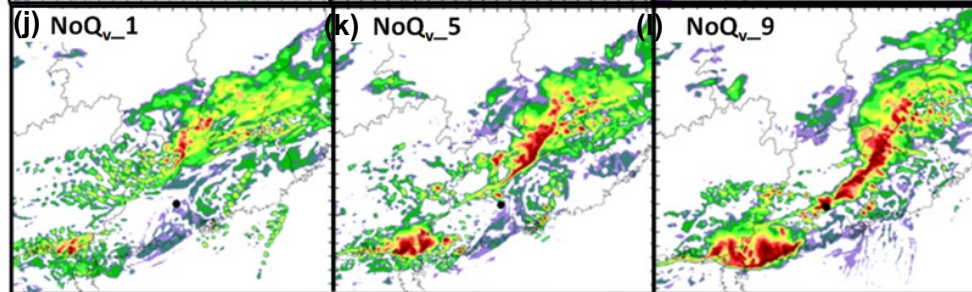
Only T



Only Qv

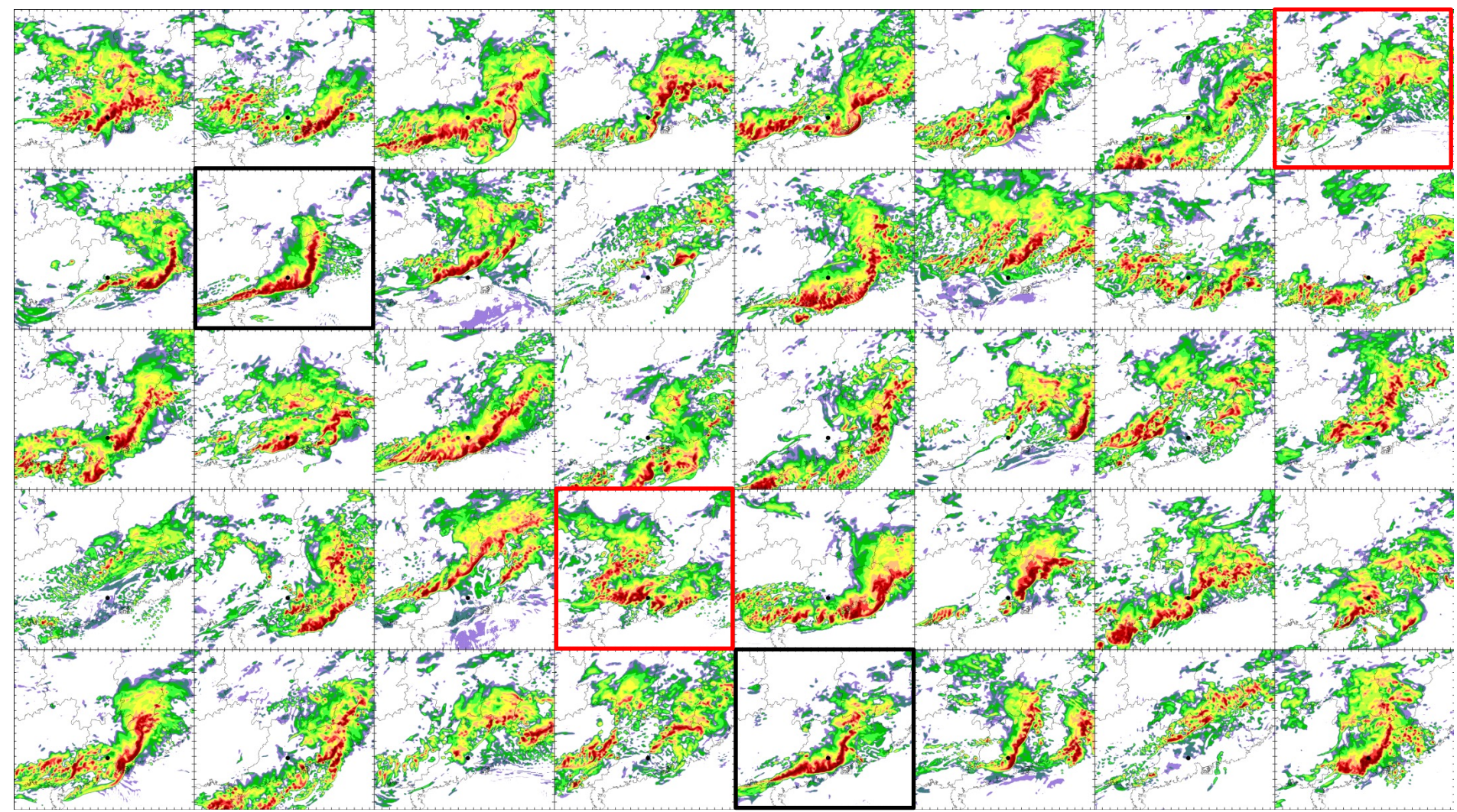


All but Qv





# Sensitivity to the initial error: different pairs



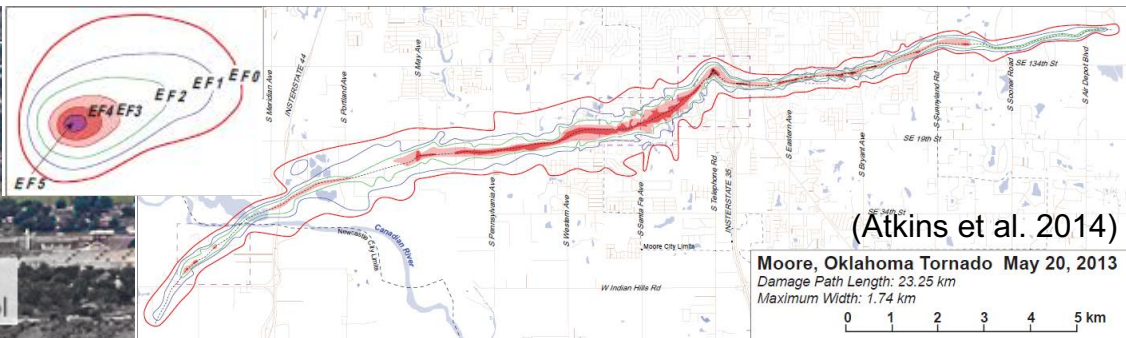
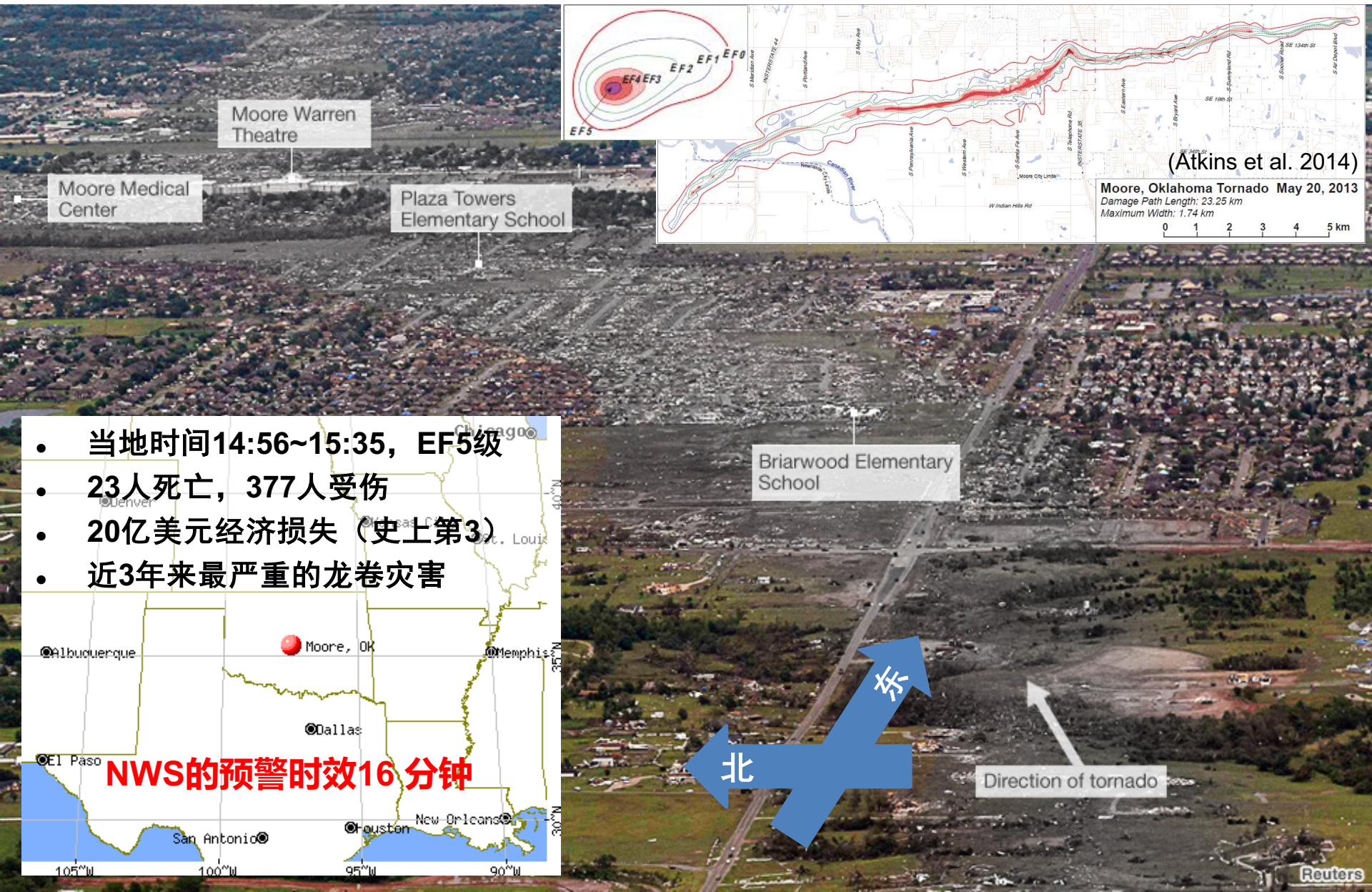
# Summary

- **Model error apparently affect the predictability of the squall line**
  - Physical parameterization
  - Grid size
  - Cumulus parameterization
- **Initial error apparently affect the predictability of the squall line**
  - Linear impact
  - The moisture condition and moist processes played an important role



# 个例2：强对流雷暴过程

# 2013年5月20日穆尔（Moore）强龙卷



- 当地时间14:56~15:35, EF5级
- 23人死亡, 377人受伤
- 20亿美元经济损失 (史上第3)
- 近3年来最严重的龙卷灾害

**NWS的预警时效16分钟**



# 造成龙卷的雷暴天气的可预报性

以2013年5月20日美国俄克拉荷马州造成穆尔强龙卷的雷暴天气过程为基础考察

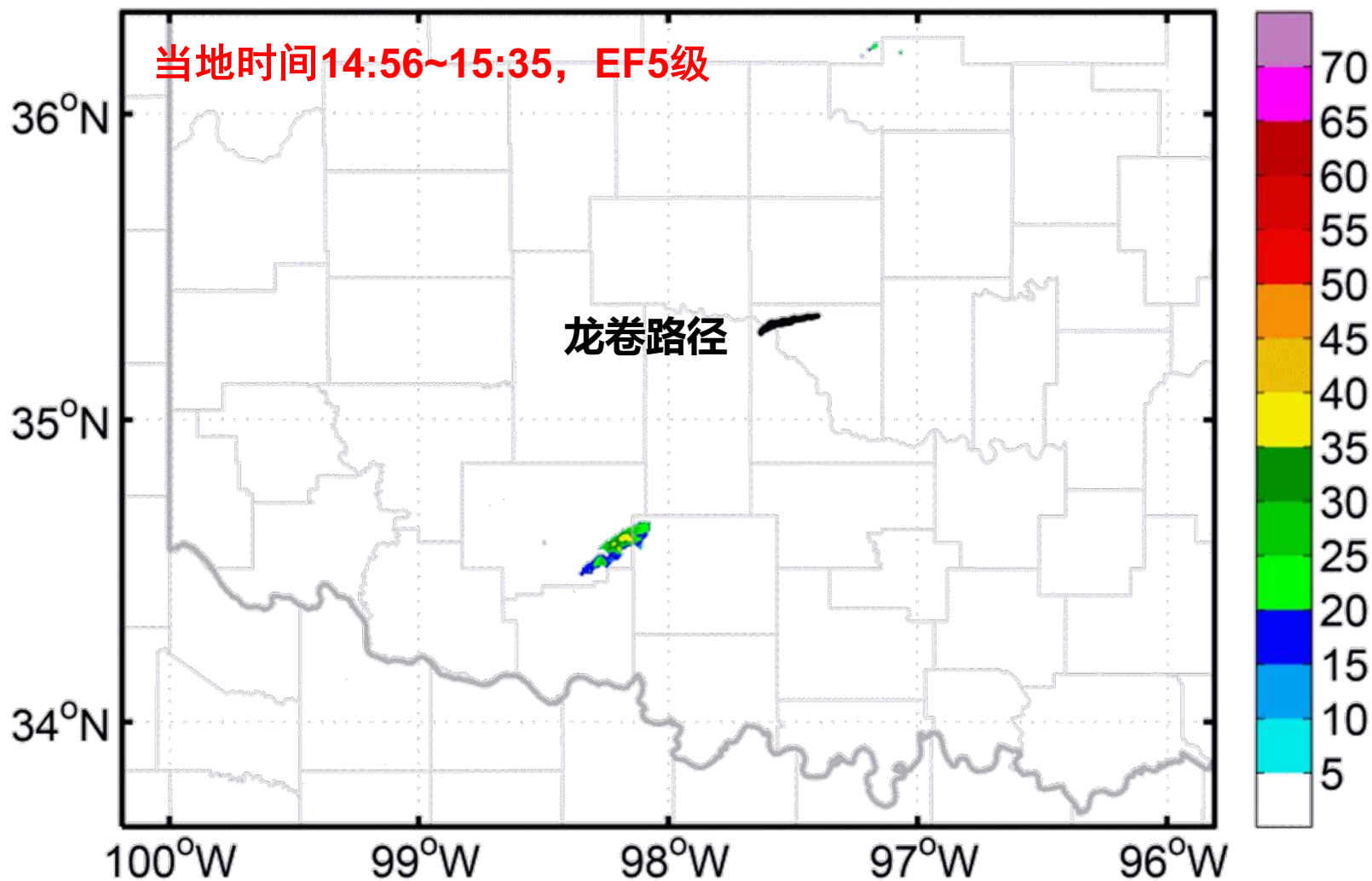
- 两种**常见实际误差来源**如何影响其**实际可预报性**
  - 初始场中天气背景条件的提前或滞后
  - 对流触发的误差
- **微小的初始误差**如何影响其**本性可预报性**
  - 减小初始误差是否能够提高预报技巧
  - 不同尺度中的误差增长特征
  - 导致误差增长的物理过程

Zhang Y., F. Zhang, D. Stensrud, and Z. Meng\*, 2015: Predictability of the Tornadoic Thunderstorm Event in Oklahoma on 20 May 2013: Sensitivity of Convection Initiation and Organization to Small Changes in Synoptic Timing and Topographical Forcing, Monthly Weather Review, 143, 2973-2997



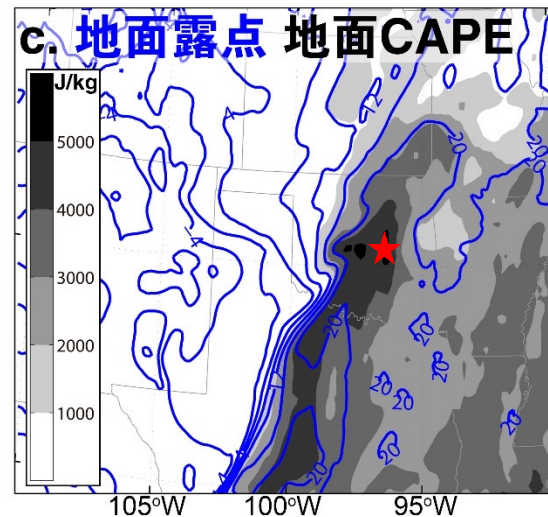
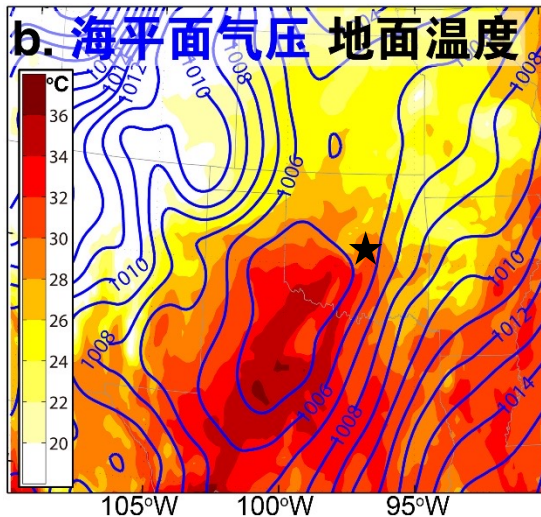
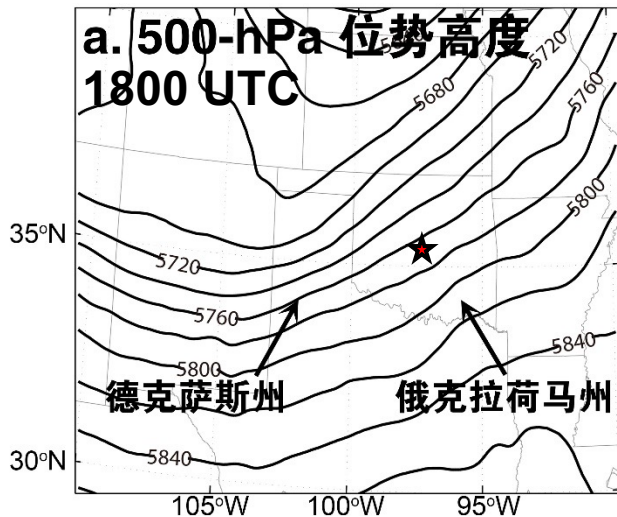
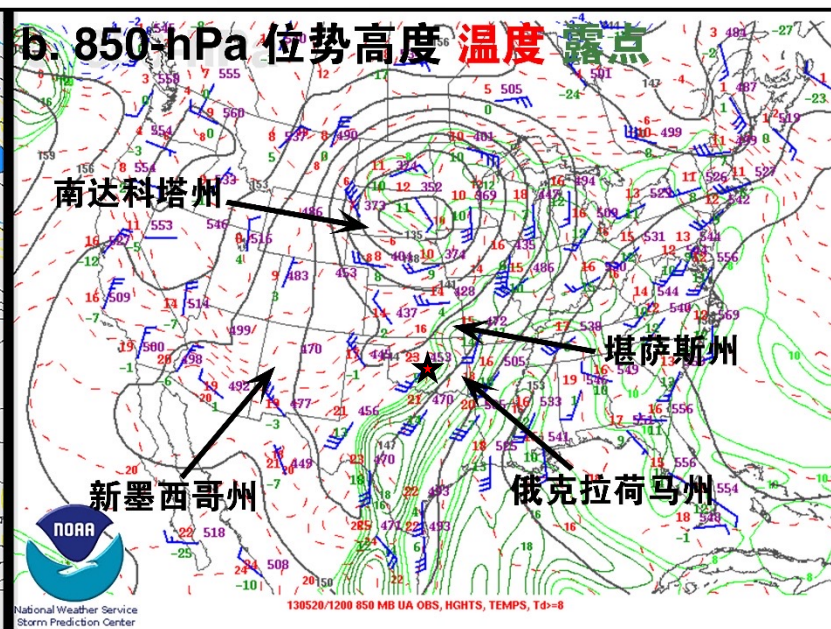
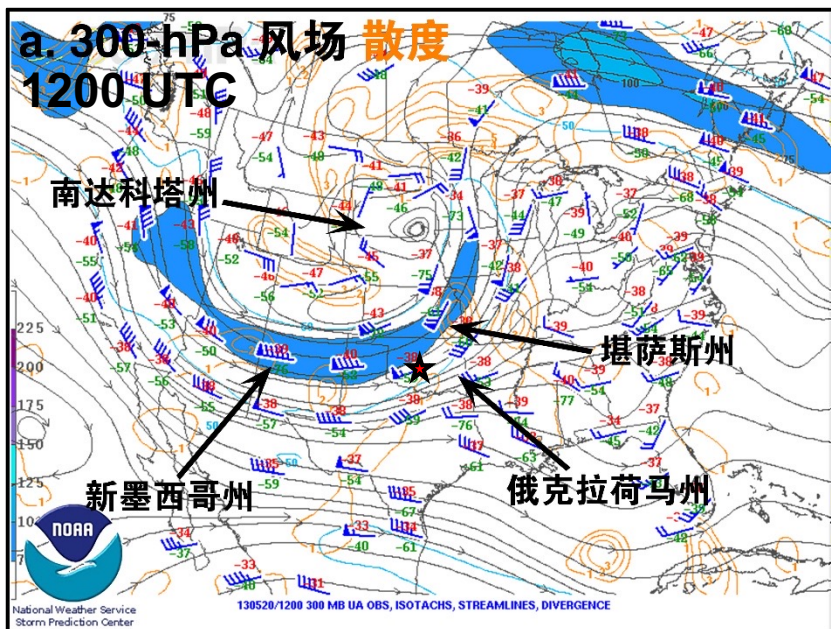
# 生成龙卷的强对流雷暴过程

Composite\_Reflectivity\_20130520180000



# 天气背景

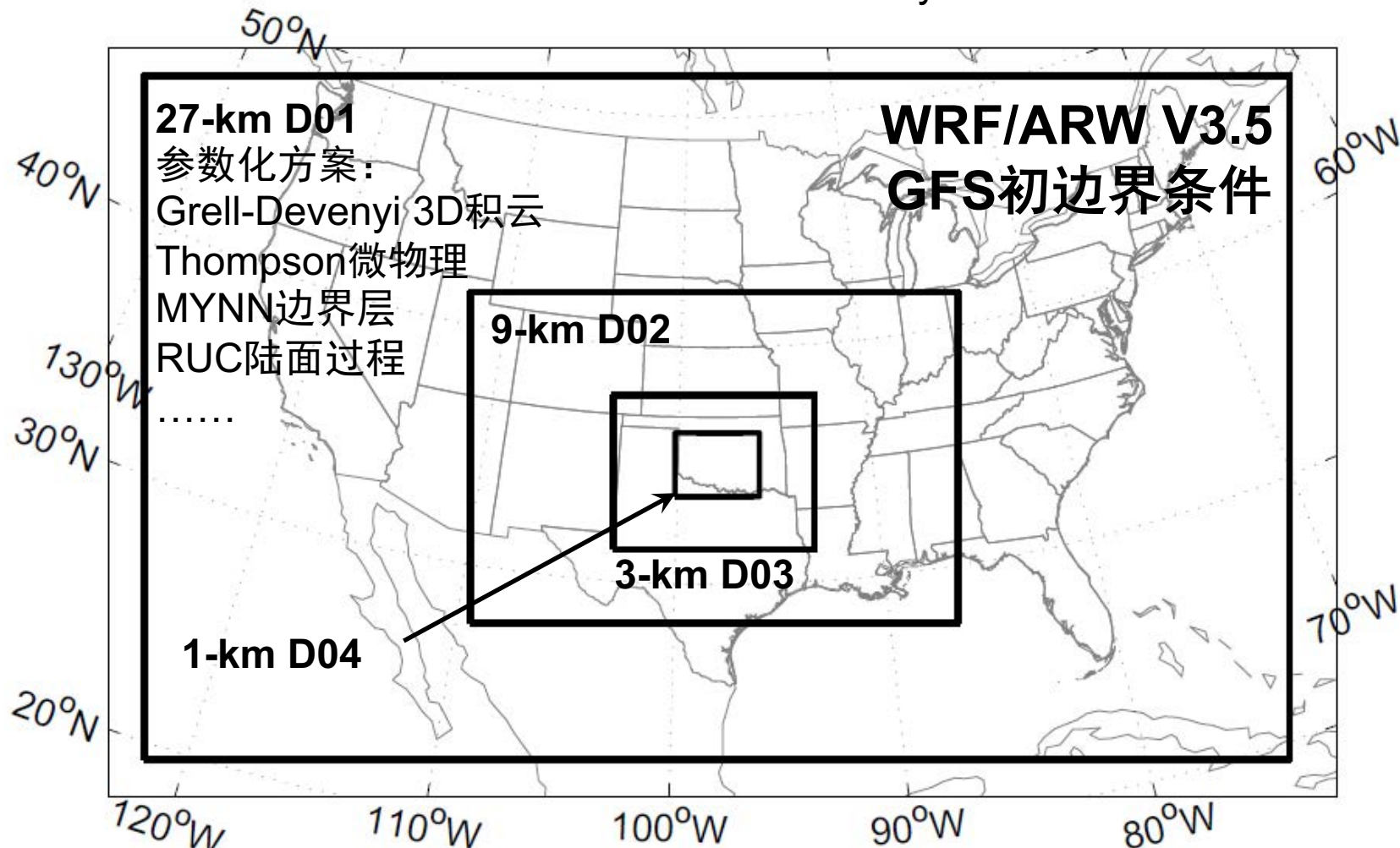
CDT=UTC-0500





# 数值模式设置

“one-way nested”



D01	D02 & D03	D04	1956~2035
-----	-----------	-----	-----------

5月19日  
1200 UTC

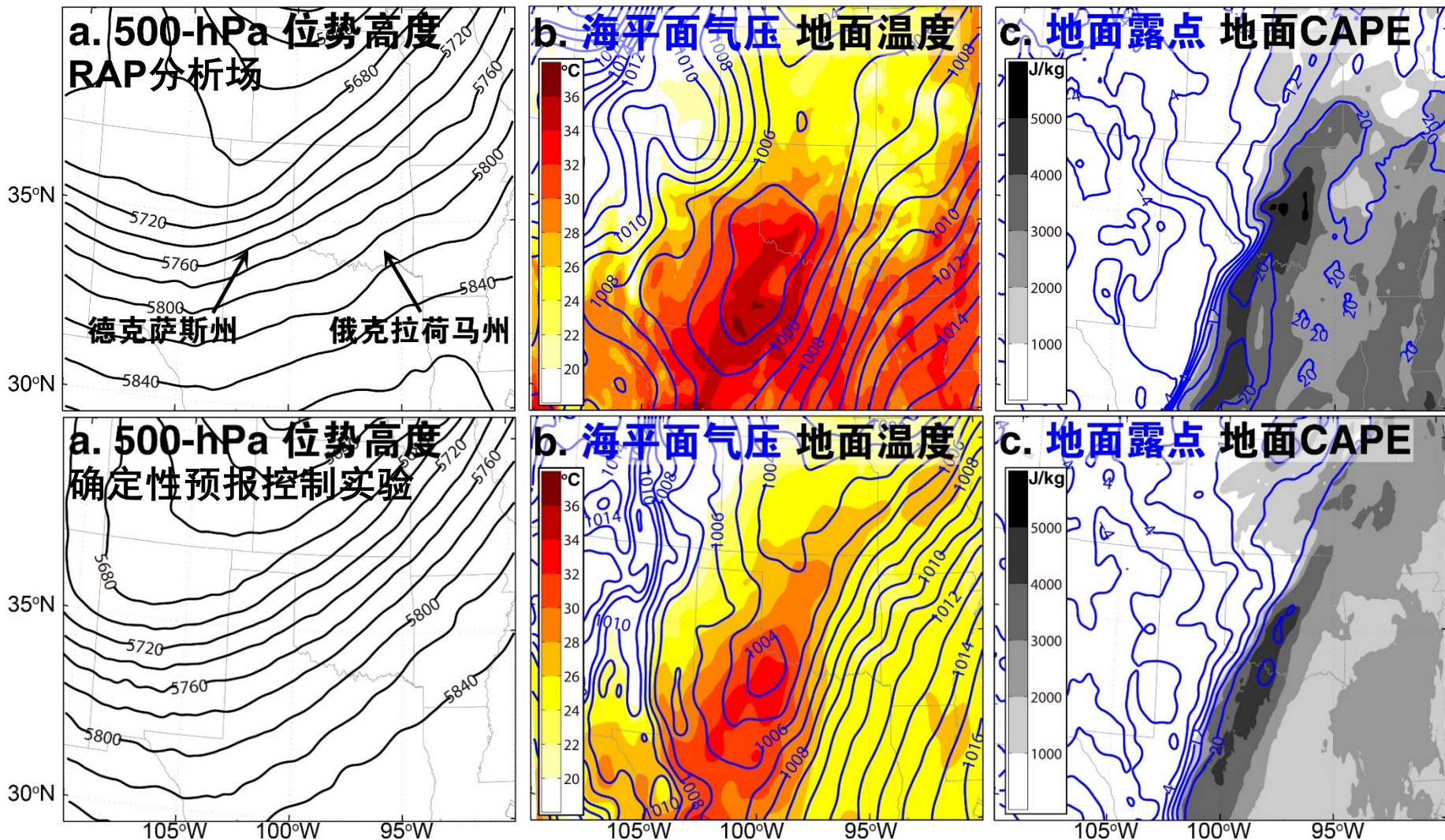
5月20日  
1200 UTC

5月20日  
1500 UTC

**龙卷**

5月21日  
0000 UTC

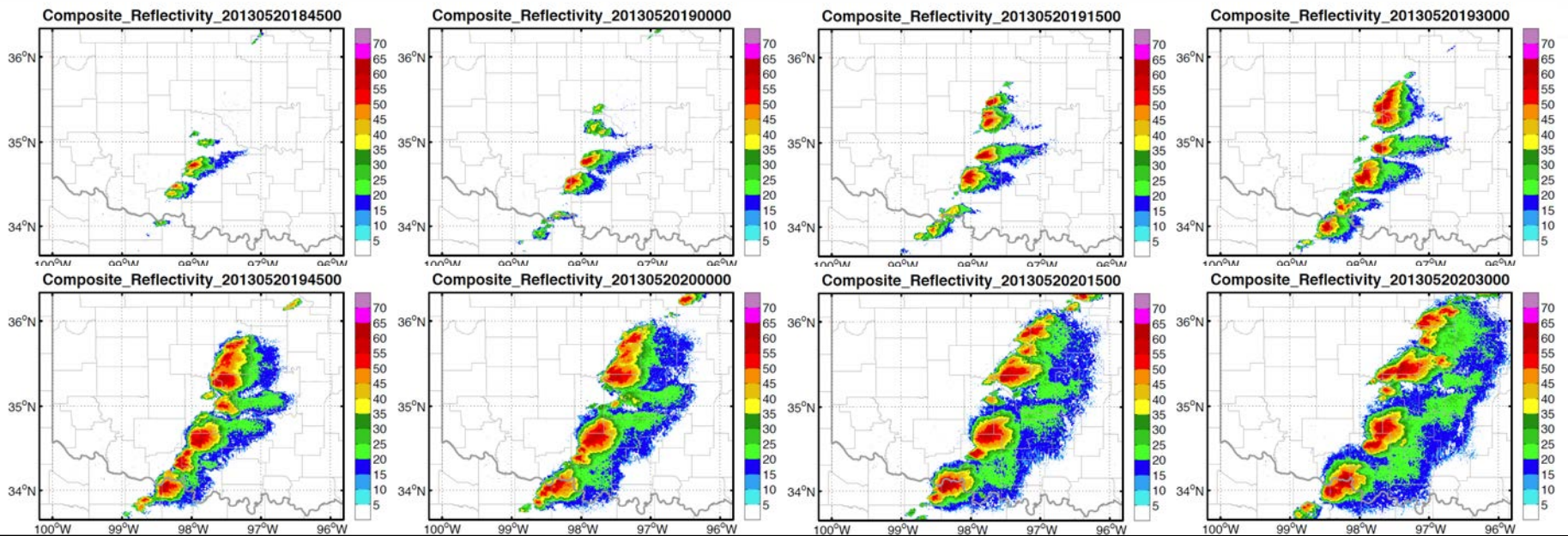
# 数值模式对天气背景条件的模拟



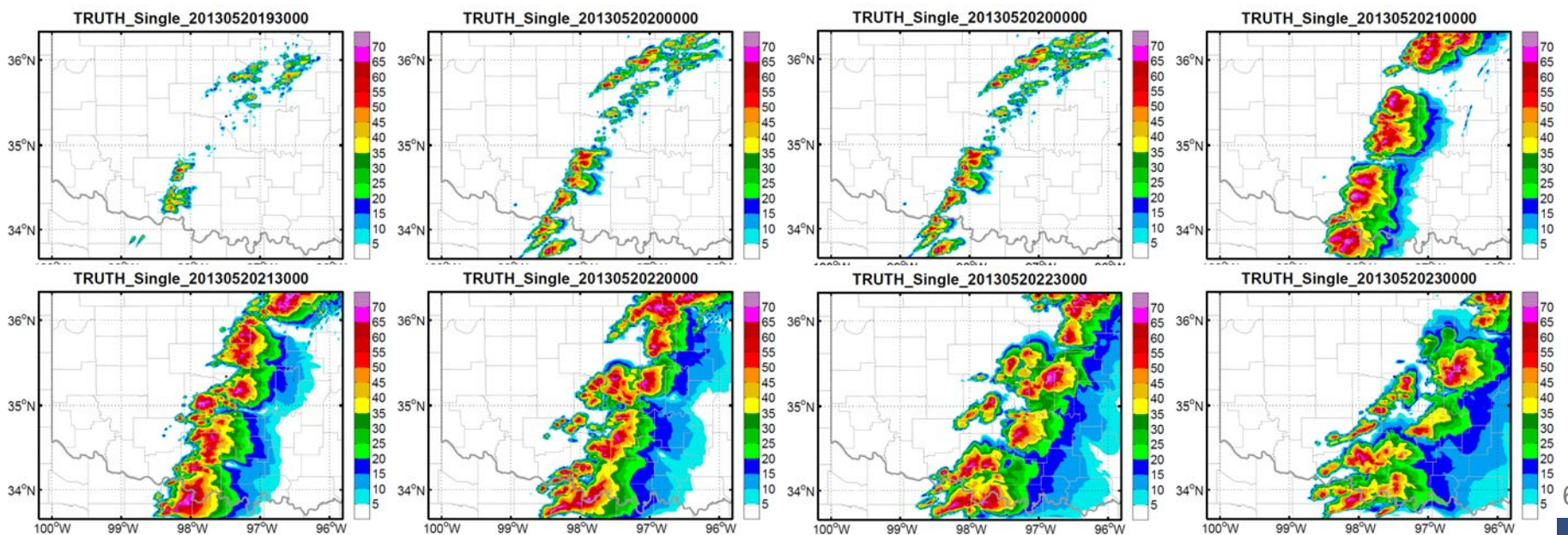


# 确定性预报控制实验模拟的雷暴

观测



模拟





# 可预报性

**Predictability** is the degree to which a correct prediction or forecast of a system's state can be made, either qualitatively or quantitatively.

# 强对流雷暴预警方法的变化

- 现有预警方法：Warn-on-Detection
  - 对流环境的分析、雷达观测（中气旋、勾状回波）
  - 预警时间很难进一步提高
- 探索使用高分辨率集合预报提供灾害天气预警（Warn-on-Forecast）
- 需要了解中小尺度强对流天气的**可预报性**

# 中尺度可预报性的研究进展和局限

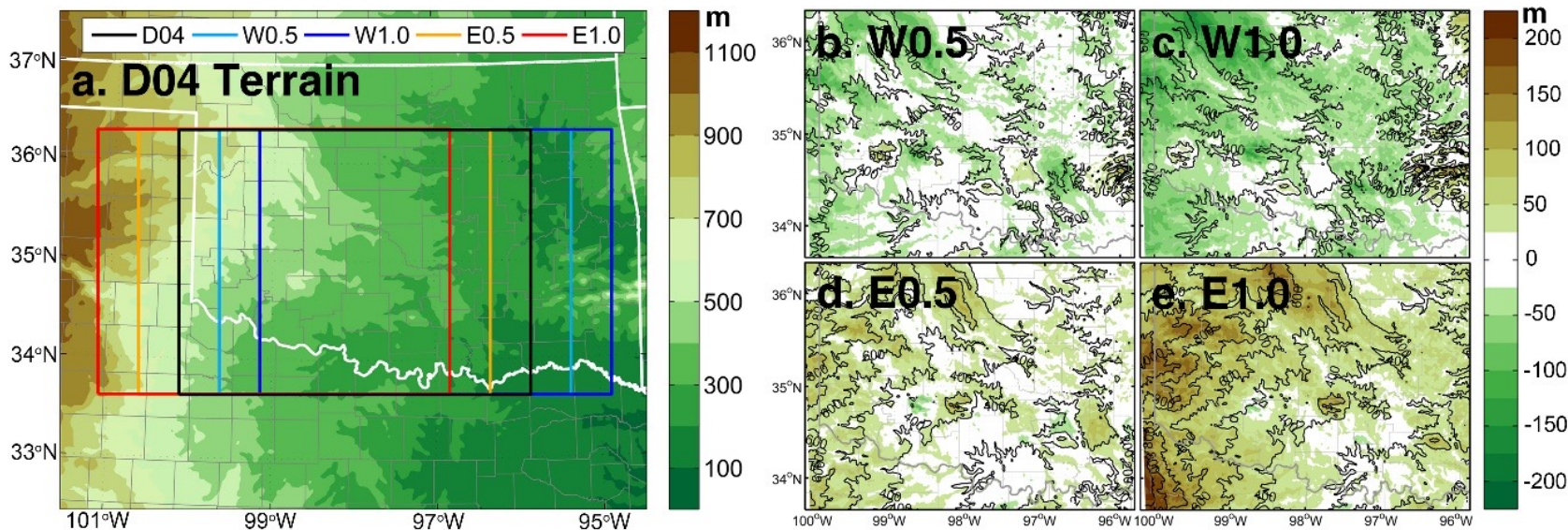
- **实际可预报性**：当前水平下对天气过程能够准确预报的最长时限
  - 多集中于中 $\alpha$ 和中 $\beta$ 尺度
    - TC: Sippel et al. (2008), Zhang et al. (2014), etc.
    - MCS: Melhauser and Zhang (2012), Wu et al. (2013), etc.
  - 中 $\gamma$ 尺度（雷暴尺度）多使用理想模式，较少探讨初始场中天气条件的误差如何影响雷暴预报
- **本性可预报性**：近乎完美的数值模式和初始场对天气过程能够准确预报的最长时限
  - 湿对流系统误差饱和及升尺度增长（Zhang et al. 2007）
  - 有大量的对于TC和MCS的个例研究
  - 鲜有针对强雷暴的工作

# 实际可预报性

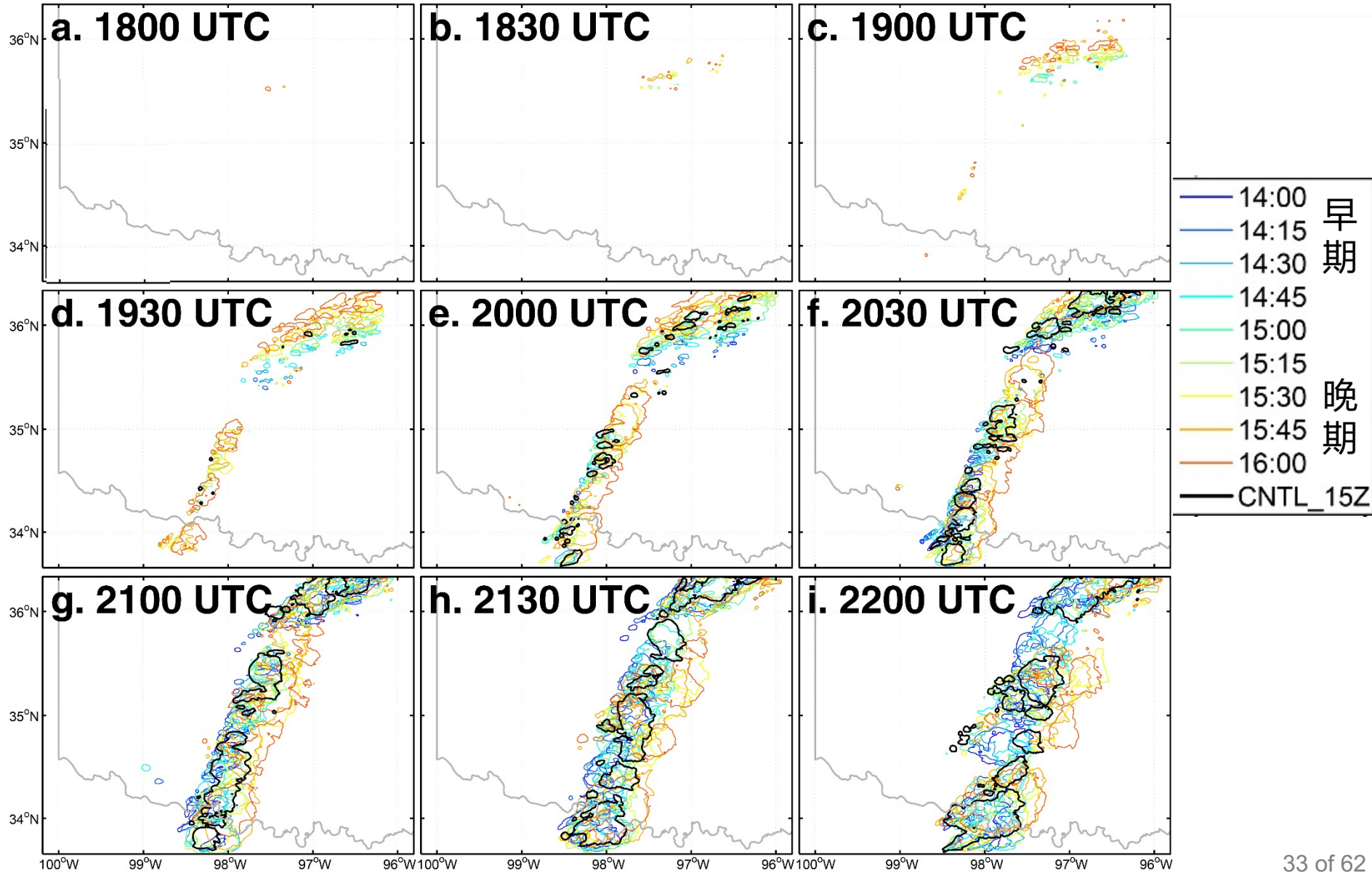
- **时间错位 (TIME\_SHIFT)** : 使用1400至1600 UTC每15分钟的模式输出作为1500 UTC时的初始场, 积分至0000 UTC



- **位置错位 (TOPO\_SHIFT)** : 将1500 UTC时初始场的下垫面地形向西或向东移动 $0.5^\circ$  或 $1.0^\circ$ , 积分至0000 UTC



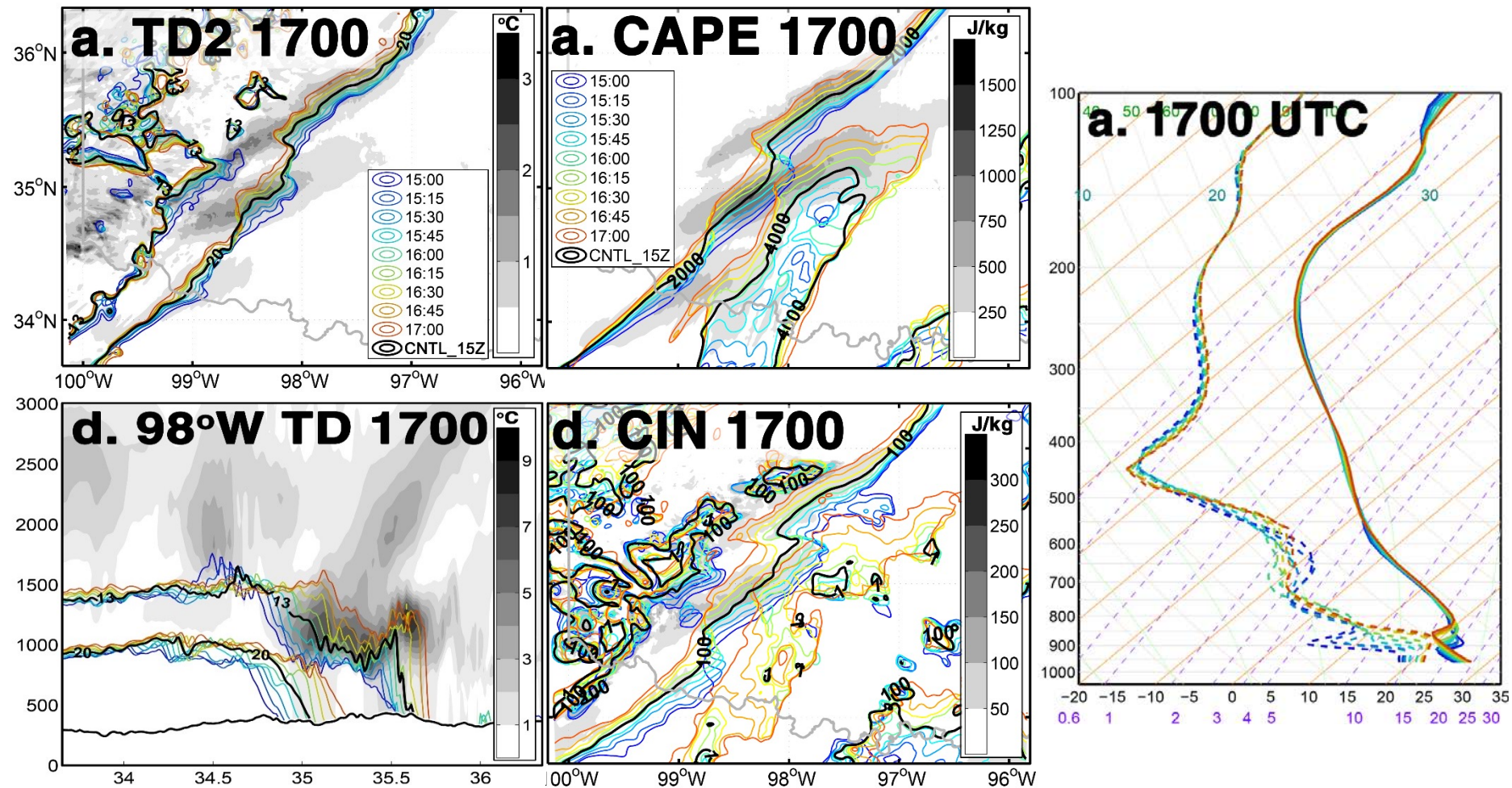
# TIME\_SHIFT的模拟结果





# 对流条件

天气背景时间对边界层的调制作用改变不同模拟的对流条件



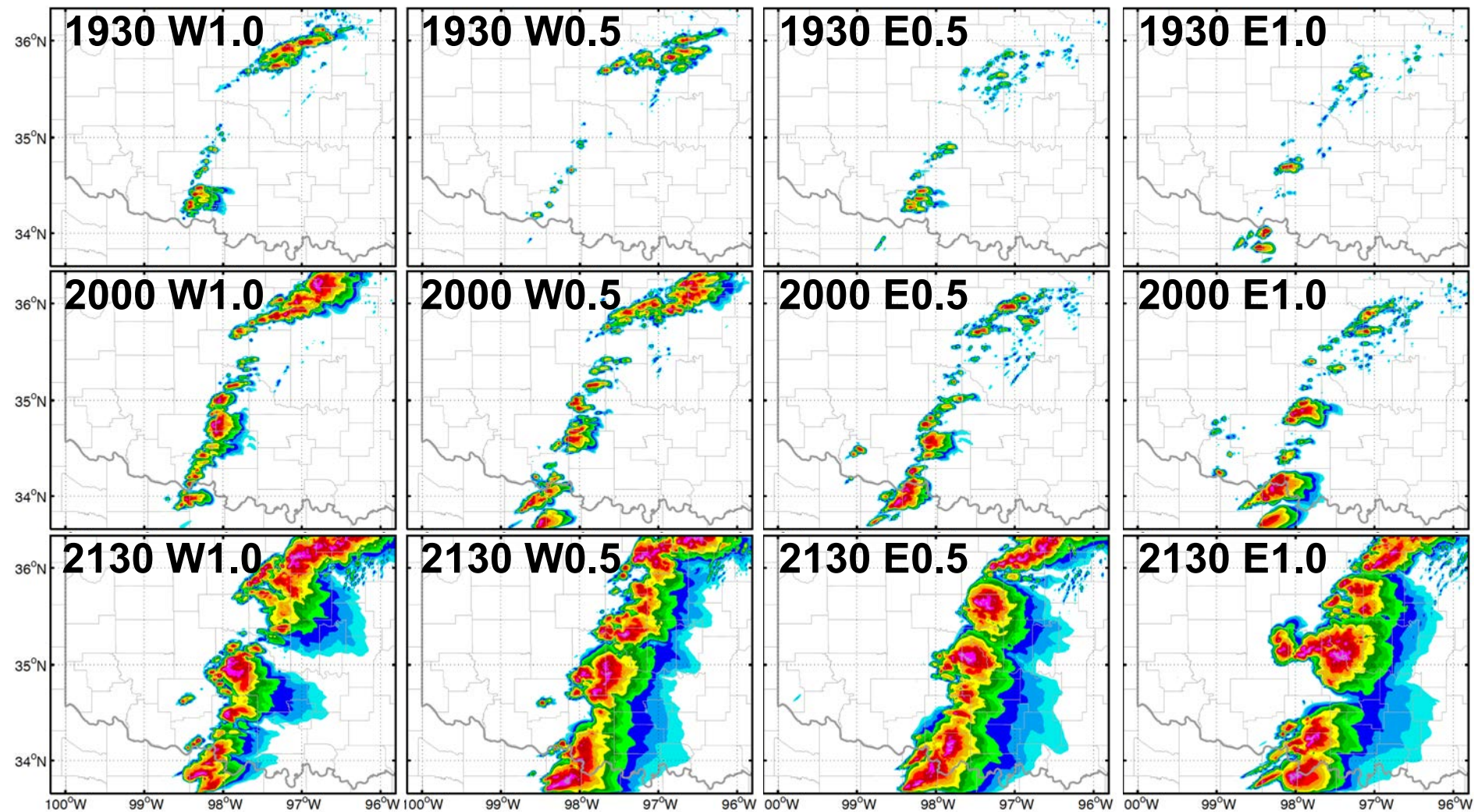
13 & 20 °C露点温度 (等值线)  
及露点温度集合发散度 (阴影)

2000 & 4000J/kg CAPE和1 &  
100J/kg CIN及集合发散度

# TOPO\_SHIFT的模拟结果

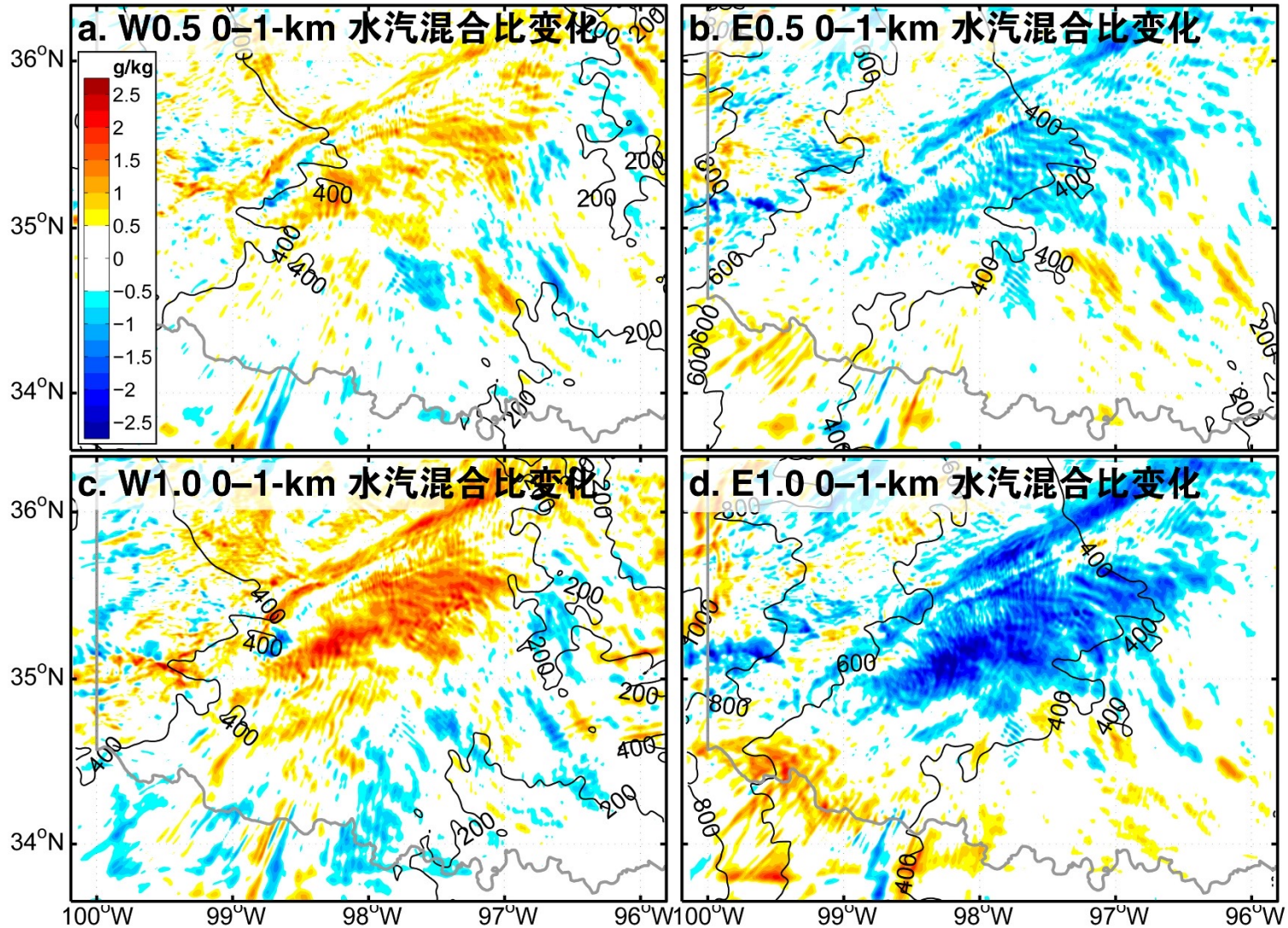
地形西移，积分区域地形降低

地形东移，积分区域地形升高





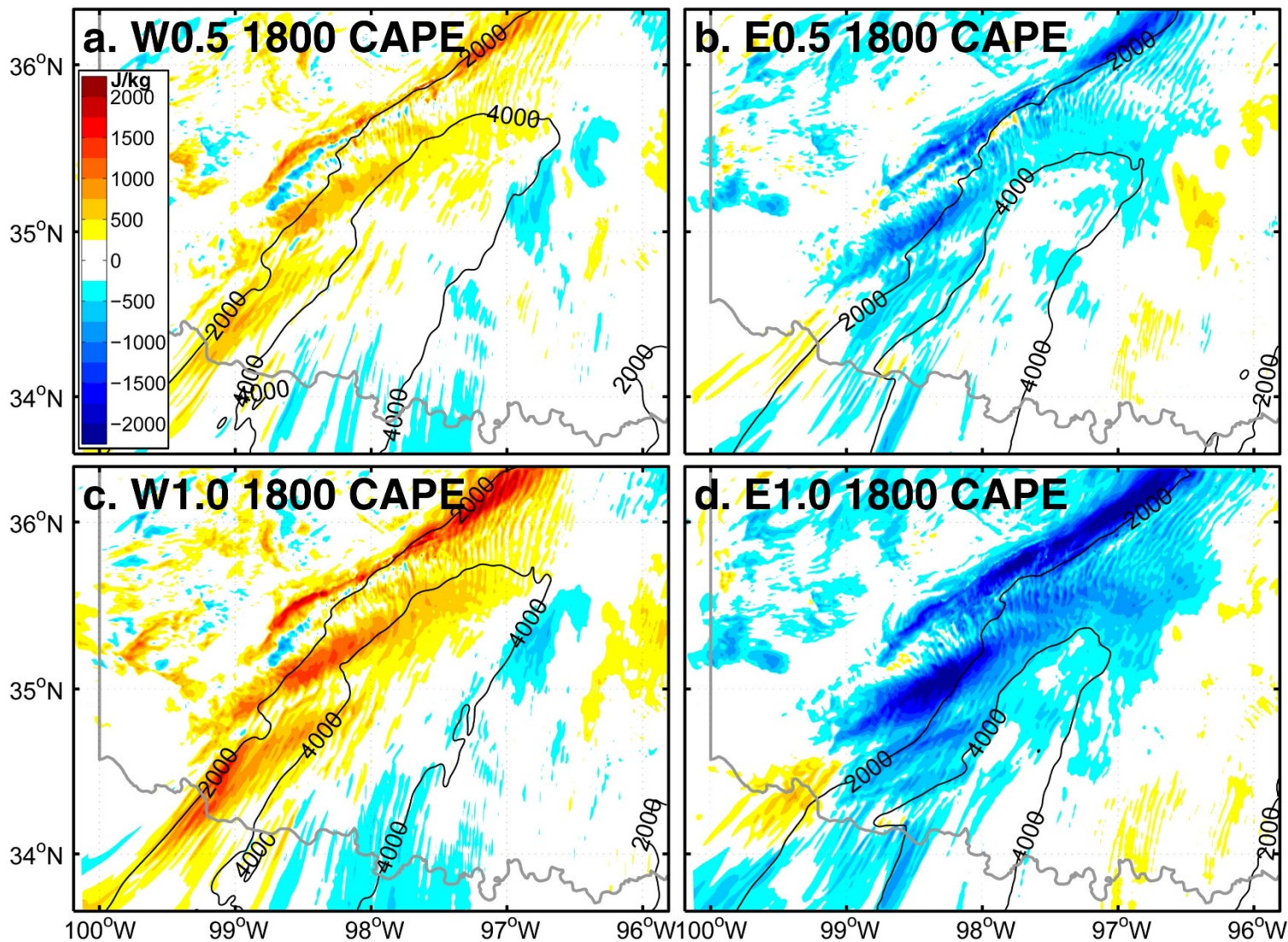
# 对流条件：水汽



1500–1800 UTC 0–1-km平均水汽变化TOPO\_SHIFT与CNTL之差

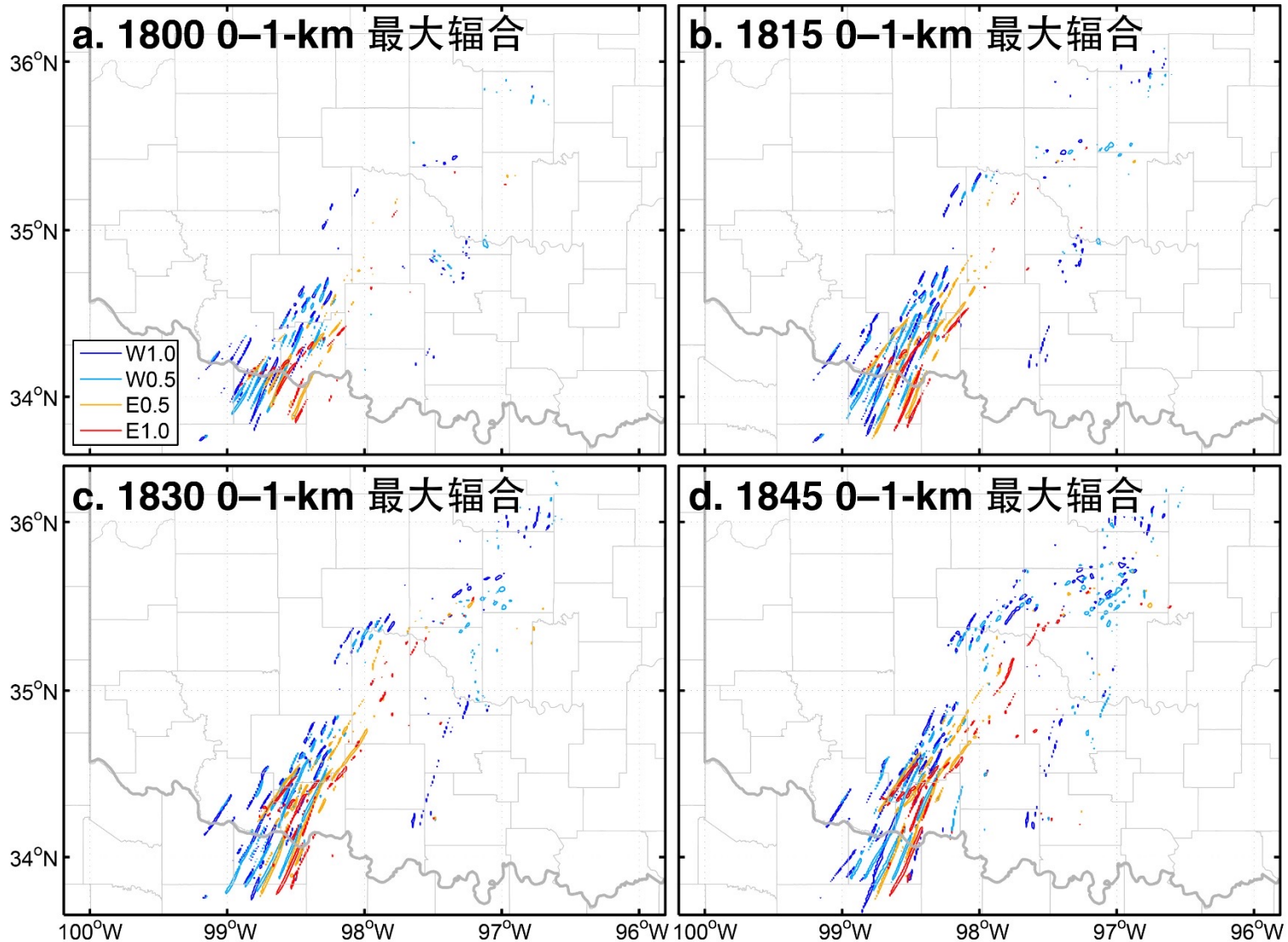


# 对流条件：不稳定性



CAPE TOPO\_SHIFT与CNTL之差

# 动力条件：低层辐合

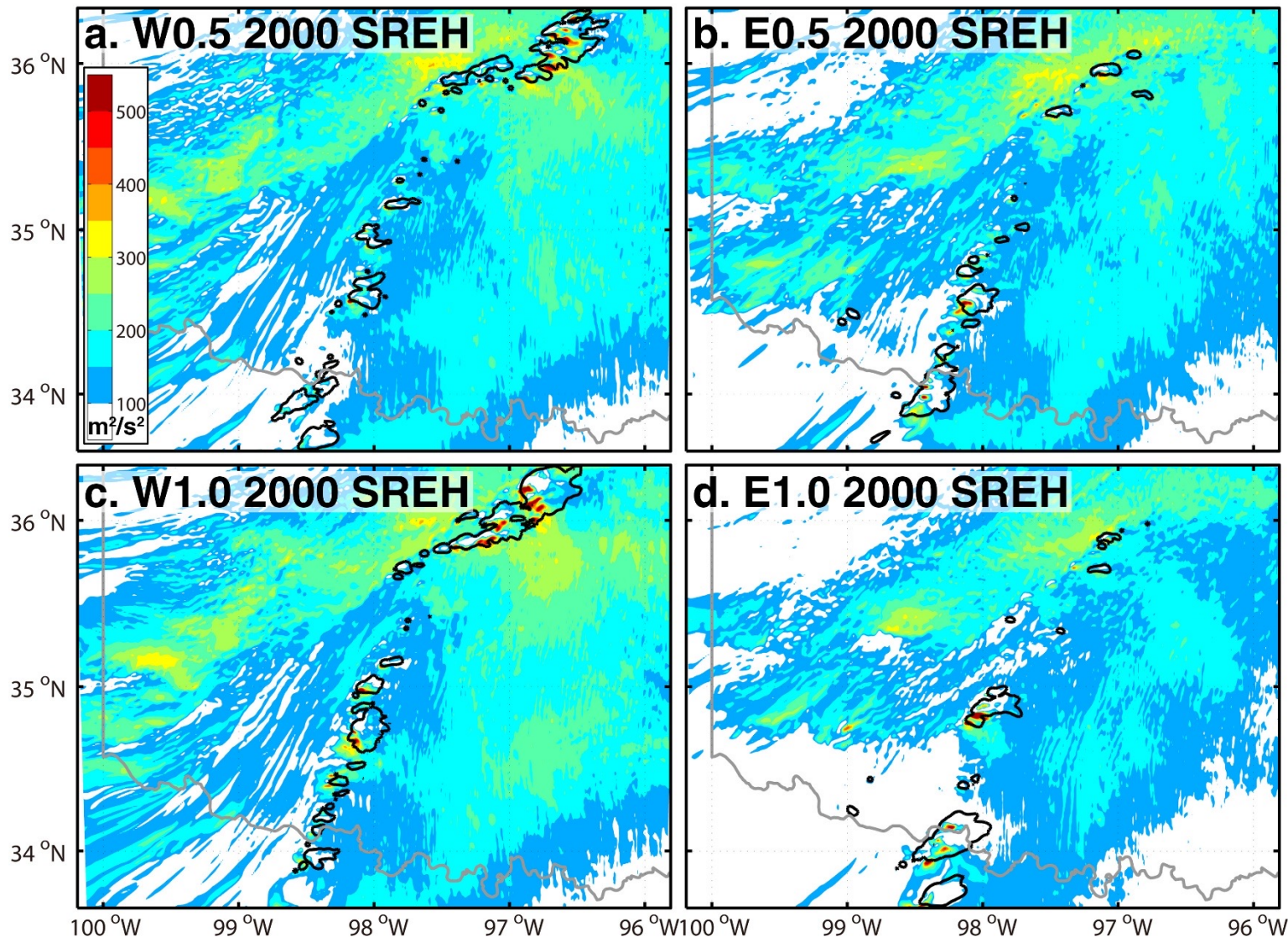


**TOPO\_SHIFT 0-1-km最大辐合 $0.0015 \text{ s}^{-1}$ 等值线**



# 动力条件：环境螺旋度

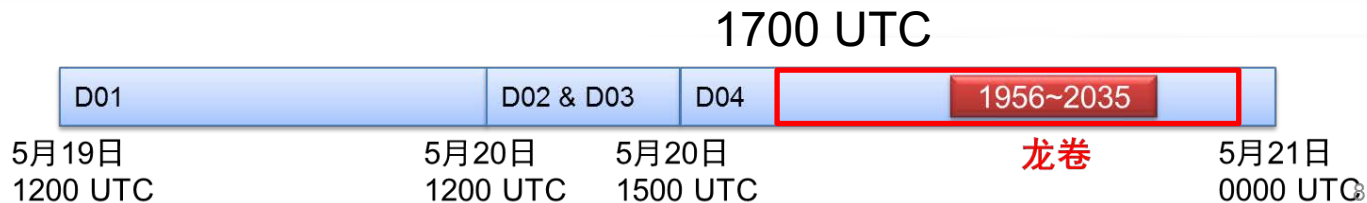
composite reflectivity (contours)



TOPO\_SHIFT雷暴相对环境螺旋度 (SREH)



# 本性可预报性

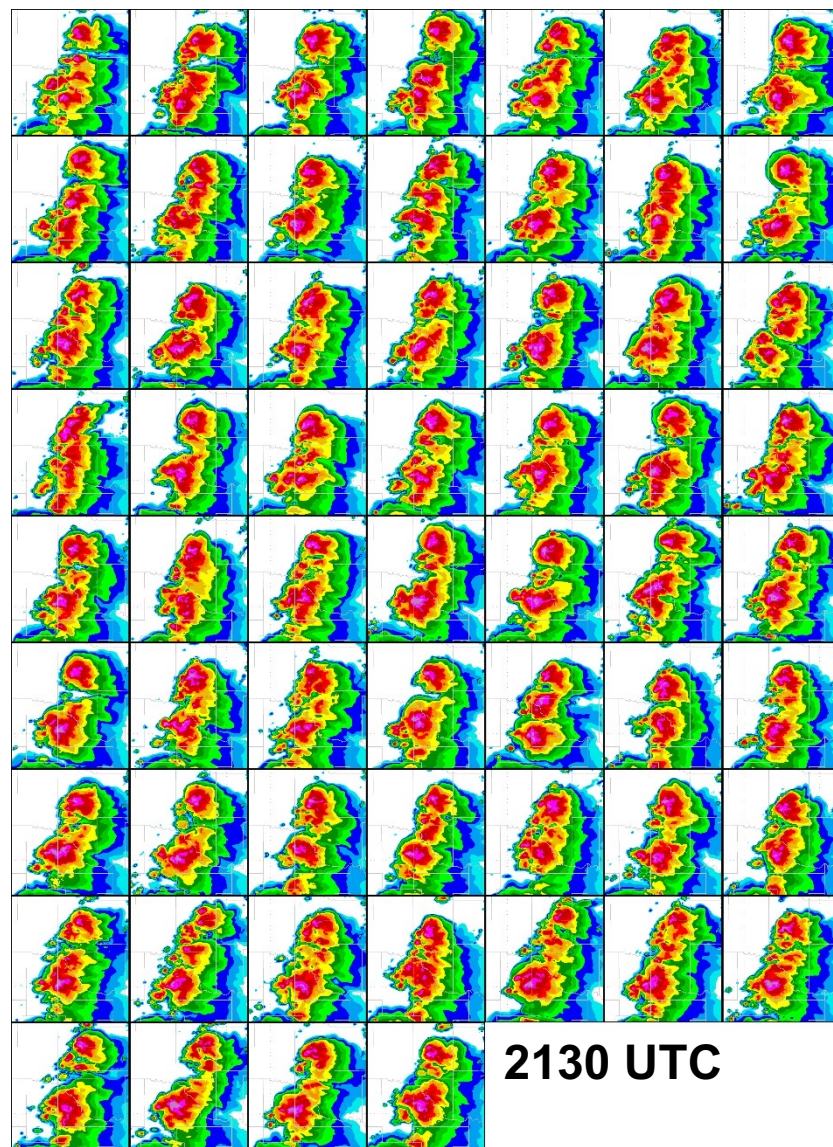
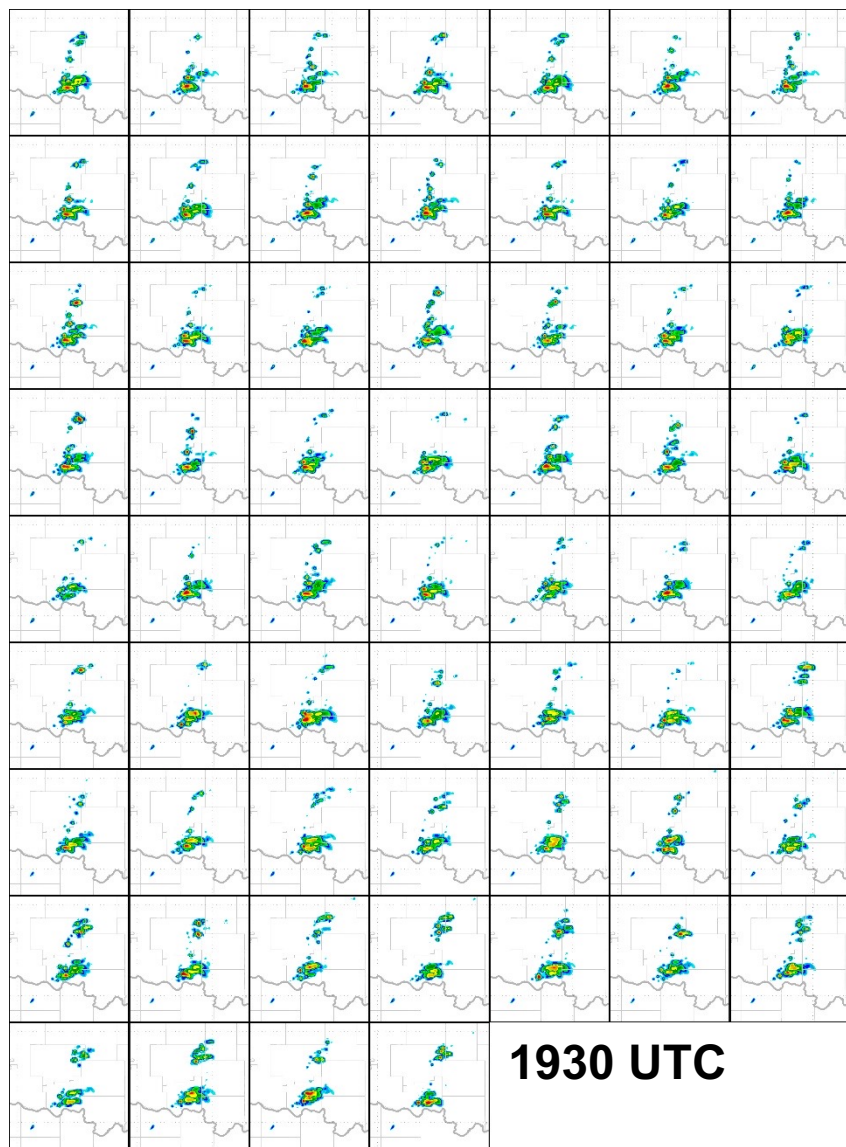


- **EF\_PERT**: 在1700 UTC时扰动生成60个集合成员的初始场，进行6小时集合预报至2300 UTC
- **EF\_TINY**: 将初始扰动缩小至10%，其余不变
- 1715 UTC时集合发散度统计特征：

		T (K)	Qv (g/kg)	U (m/s)	V (m/s)
<b>EF_PERT</b> 100%初始扰动	标准偏差	0.066	0.11	0.19	0.20
<b>EF_TINY</b> 10%初始扰动	标准偏差	0.0082	0.014	0.024	0.025

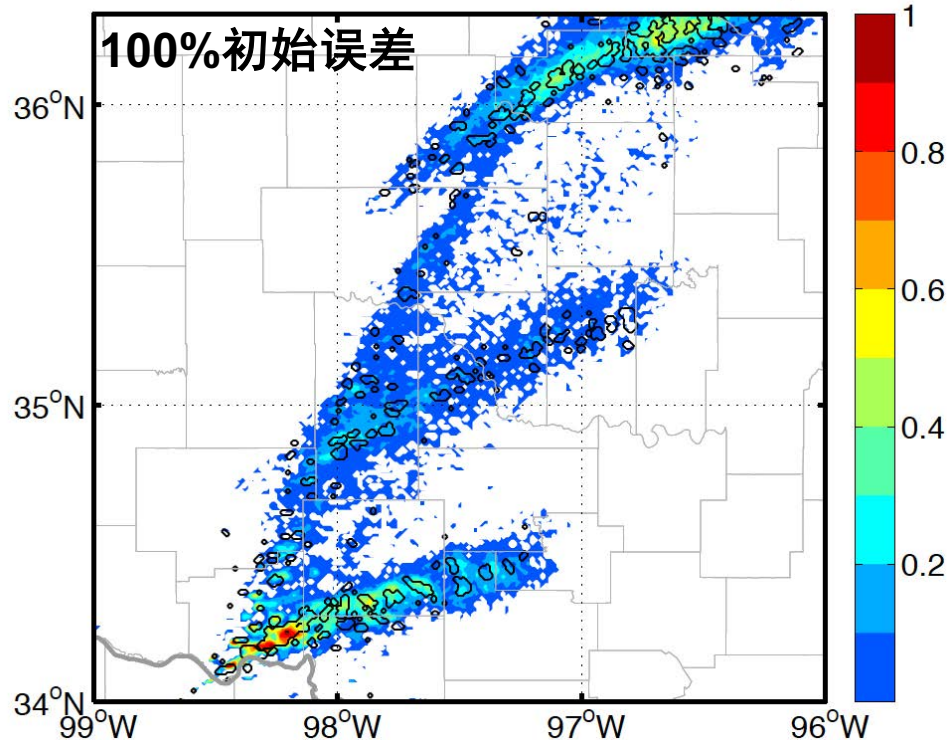
Zhang, Y., Zhang, F., Stensrud, D.J. and Meng, Z., 2016. Intrinsic predictability of the 20 May 2013 tornadic thunderstorm event in Oklahoma at storm scales. *Monthly Weather Review*, 144(4), pp.1273-1298.

# 微小初始扰动带来的预报误差

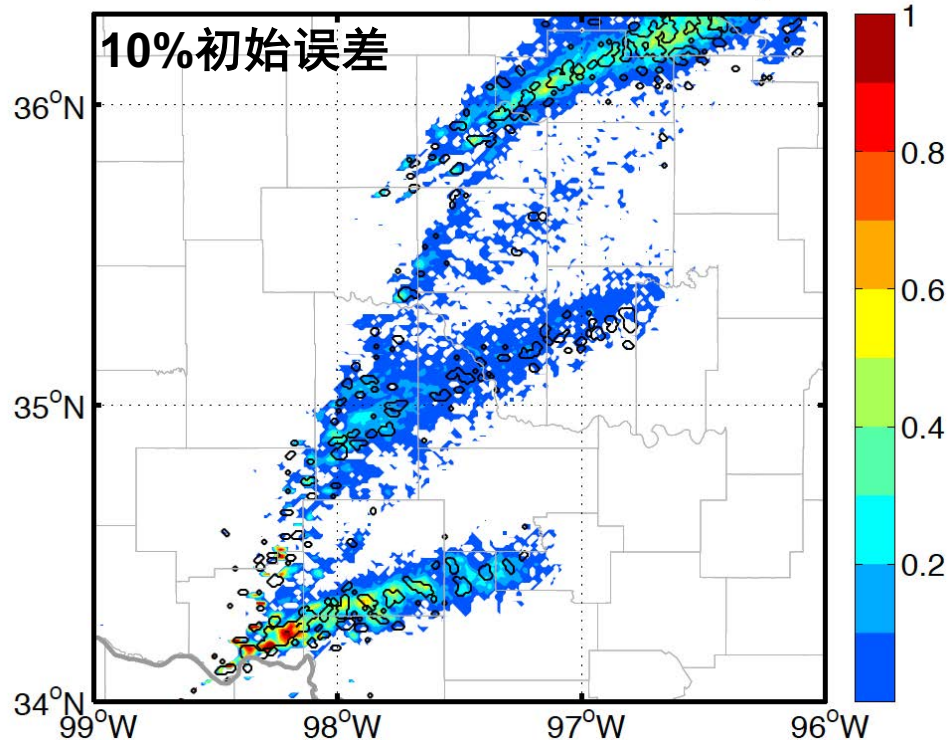


# 对中气旋位置的概率预报

EF1\_CNTL 180 m<sup>2</sup>/s<sup>2</sup> UH Probability



EF\_TINY 180 m<sup>2</sup>/s<sup>2</sup> UH Probability

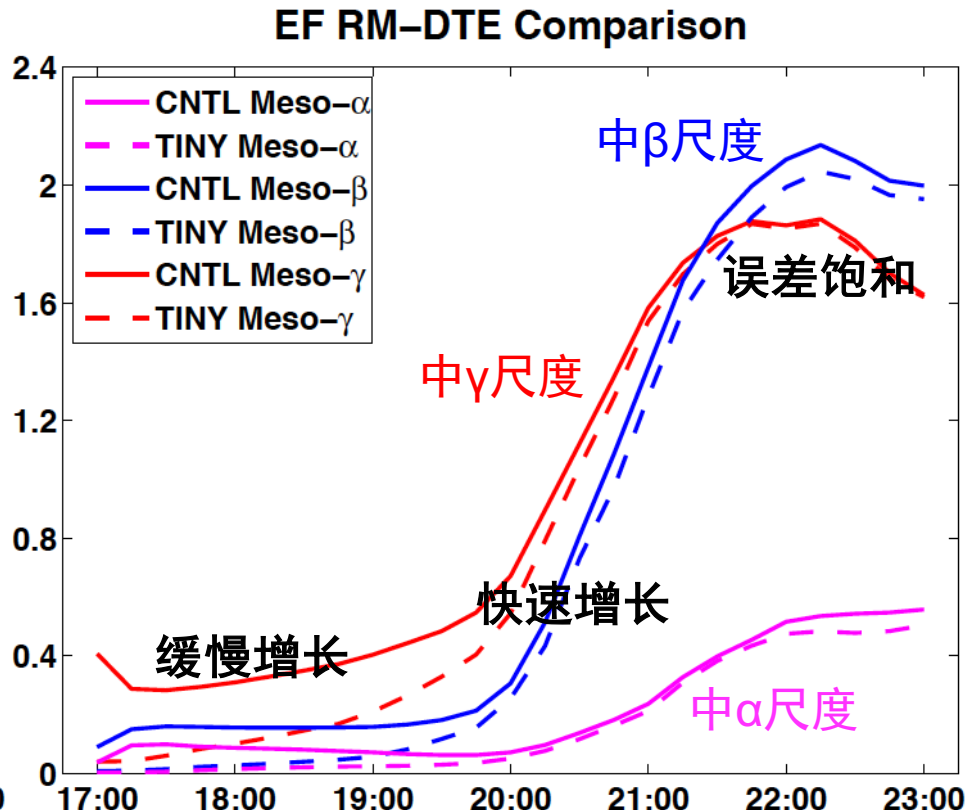
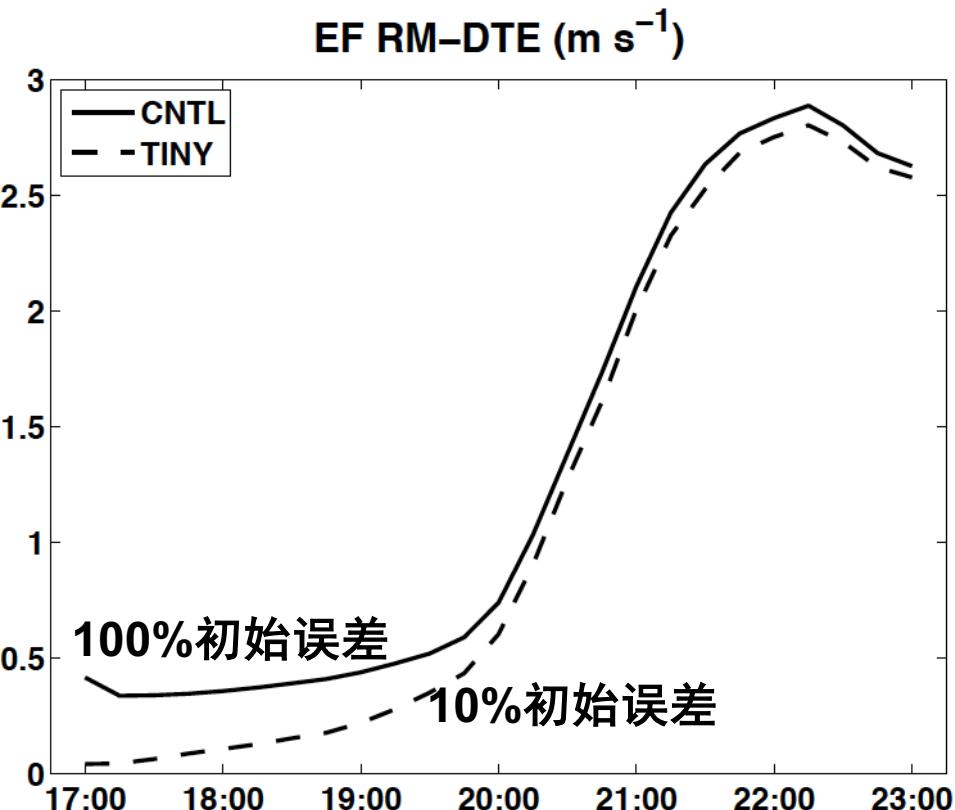


UH (updraft helicity) ,  $UH = \int_{z=2\text{km}}^{z=5\text{km}} w\zeta dz$

即使集合初始扰动减小为10%，中气旋可能的路径分布依然没有明显的变化，预报技巧并未明显提高



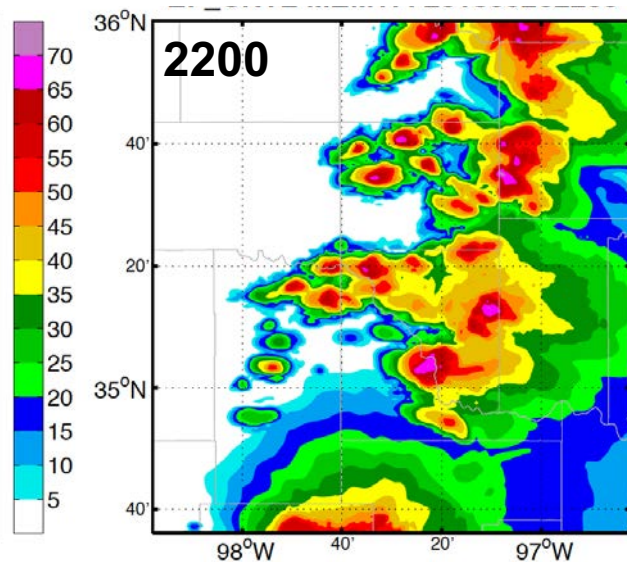
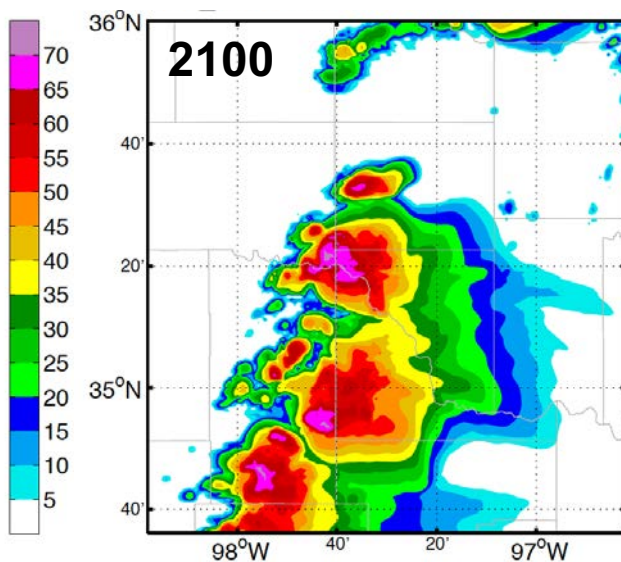
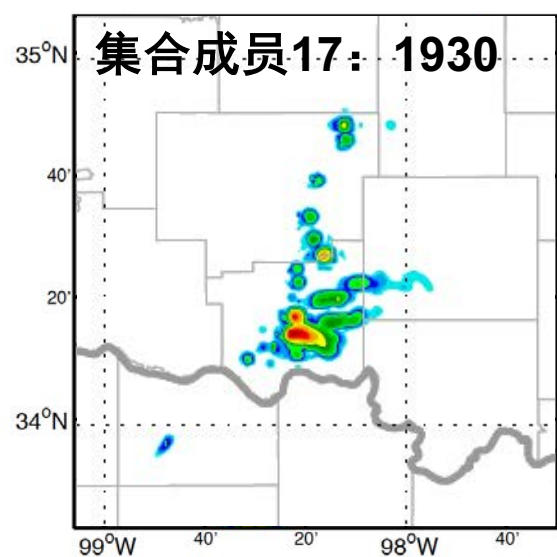
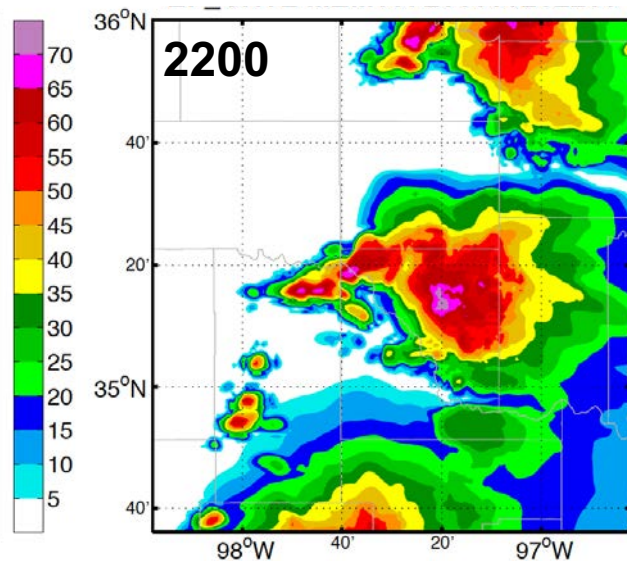
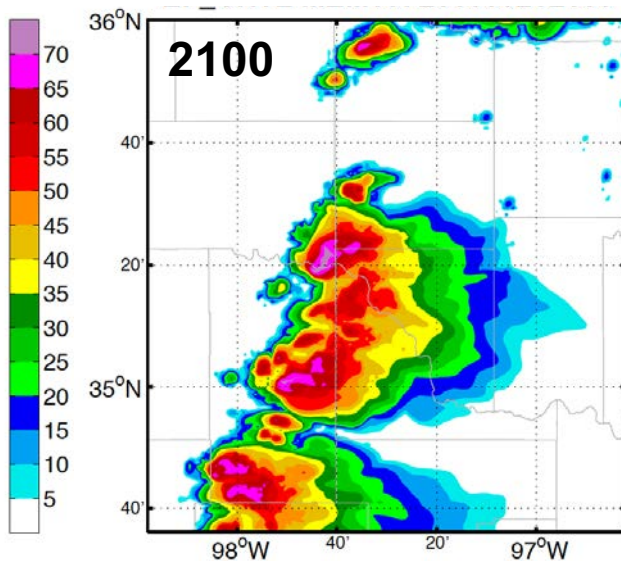
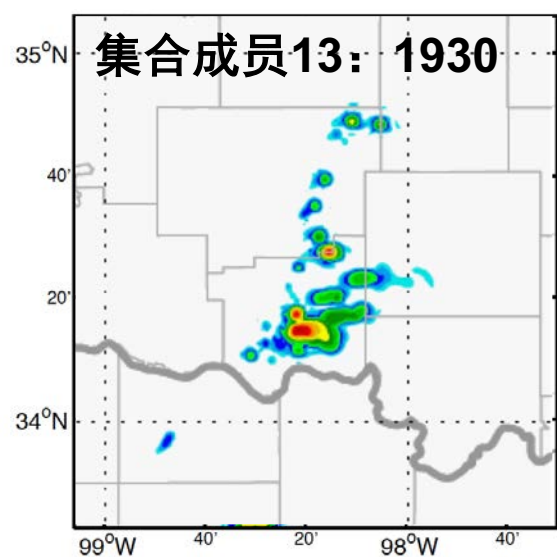
# 不同尺度的误差增长过程



$$DTE = \frac{1}{2} \left( u'^2 + v'^2 + \frac{c_p}{T_r} T'^2 \right)$$

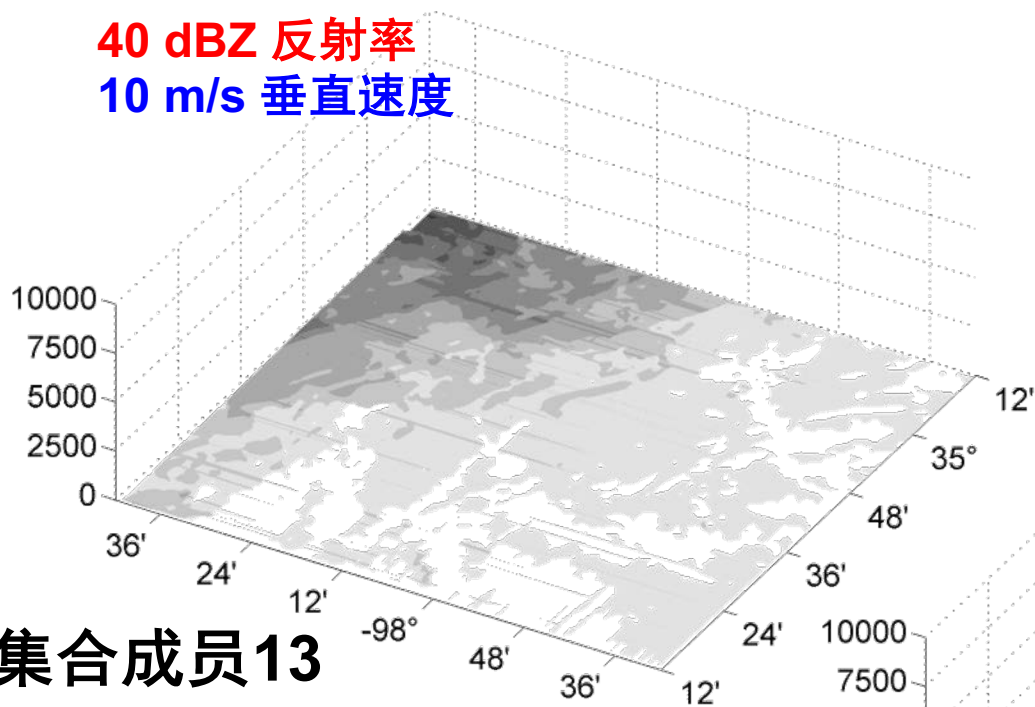
- 存在误差升尺度增长
- 深湿对流并非误差升尺度增长的必要条件
- 深湿对流会加速和放大这个过程

# 对两个集合成员的详细分析



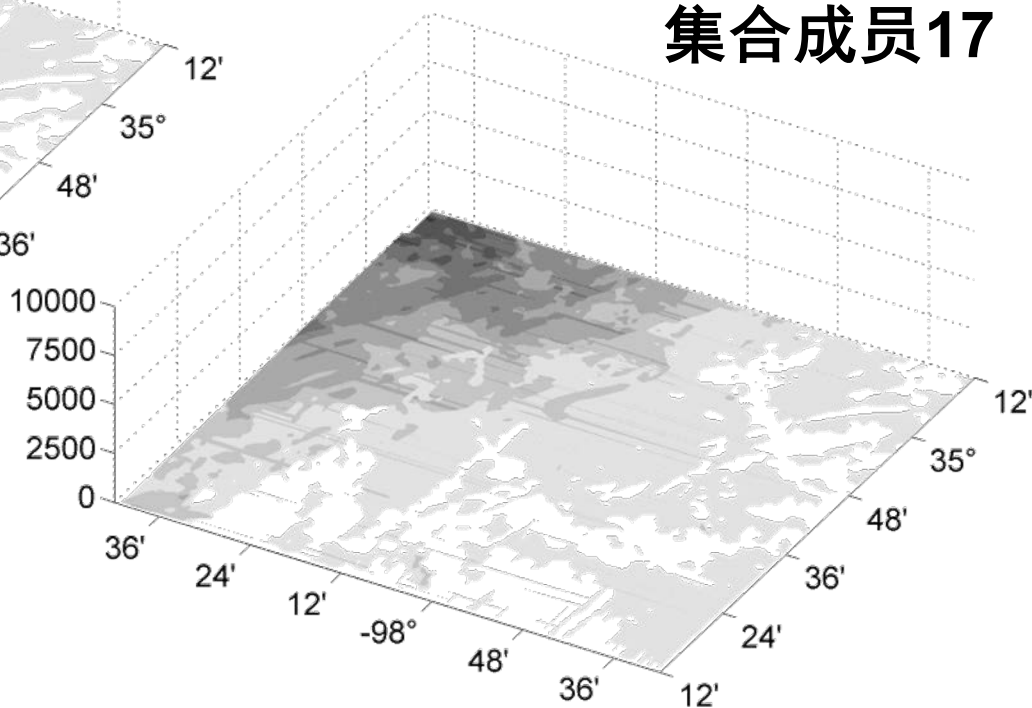
# 对流触发阶段

40 dBZ 反射率  
10 m/s 垂直速度



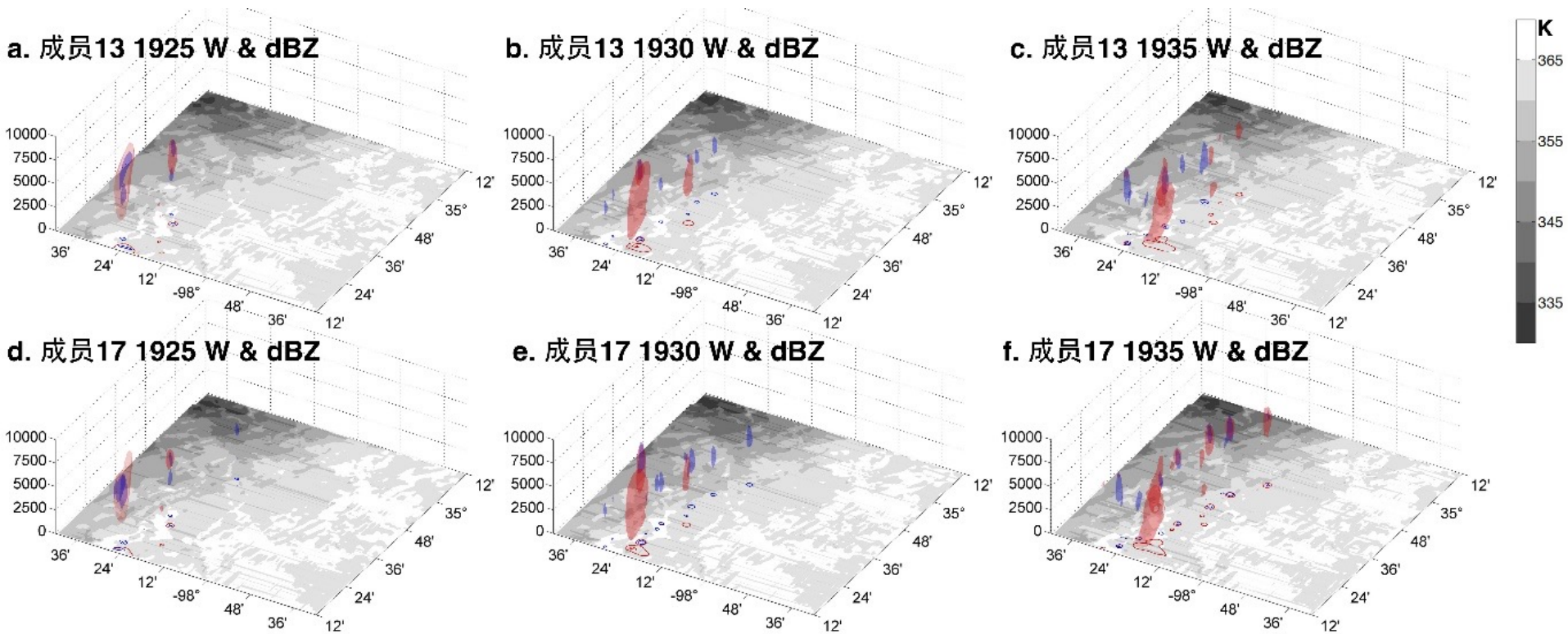
集合成员13

集合成员17





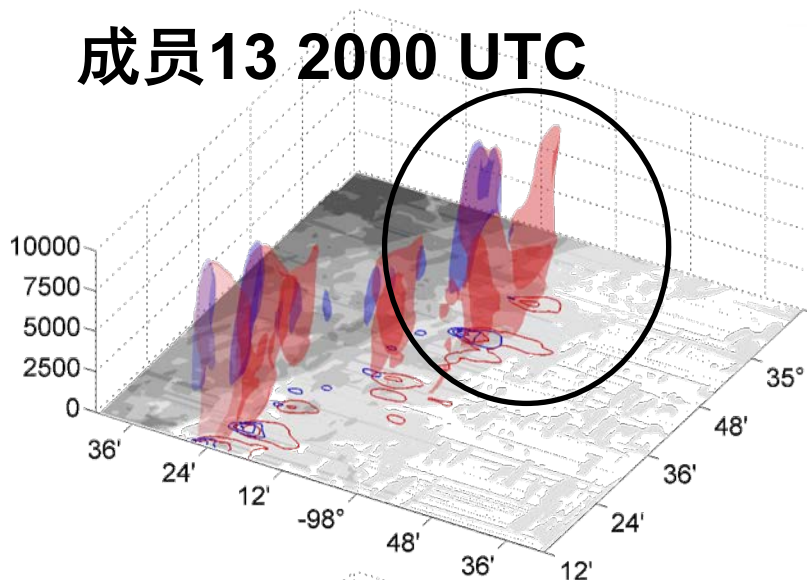
# 对流触发阶段



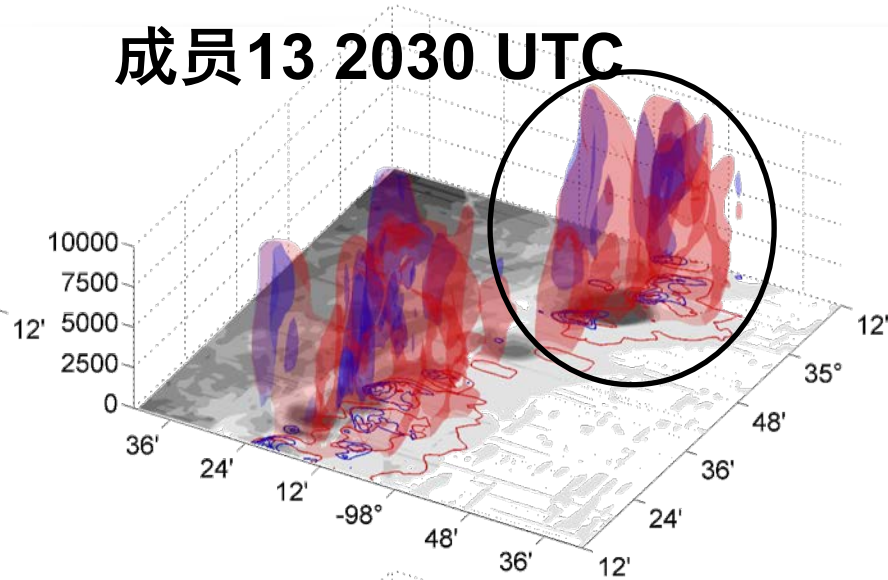
由于小尺度的湍流，对流触发的准确位置无法提前预报

# 对流的发展

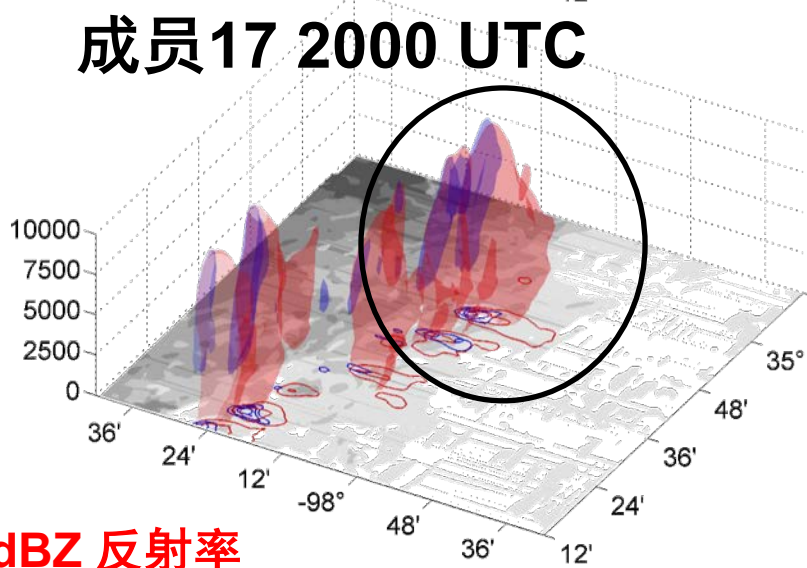
## 成员13 2000 UTC



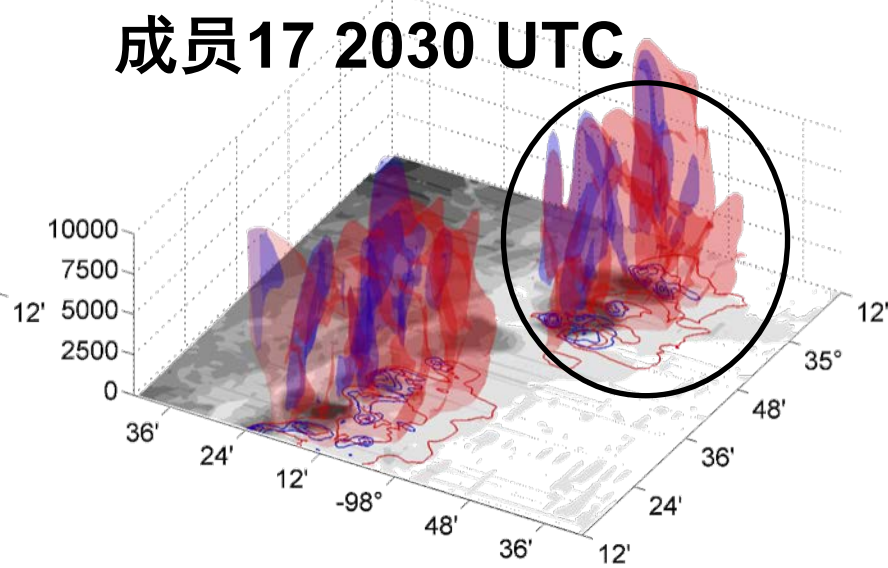
## 成员13 2030 UTC



## 成员17 2000 UTC



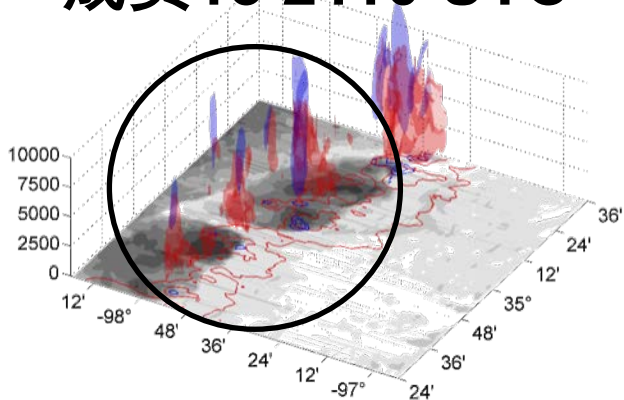
## 成员17 2030 UTC



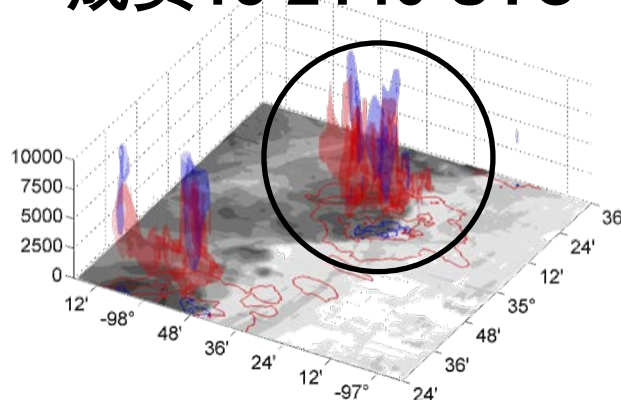
40 dBZ 反射率  
10 m/s 垂直速度

# 雷暴的组织 and 合并

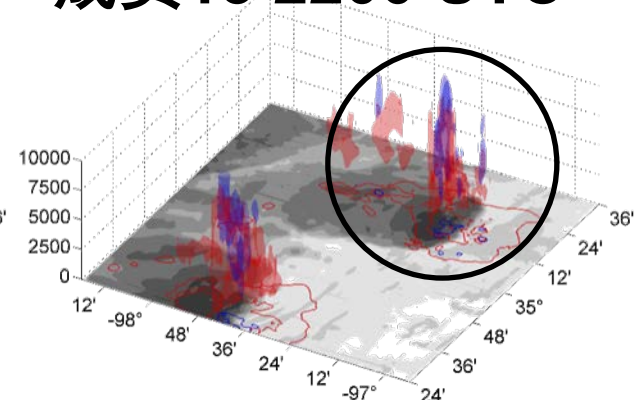
成员13 2110 UTC



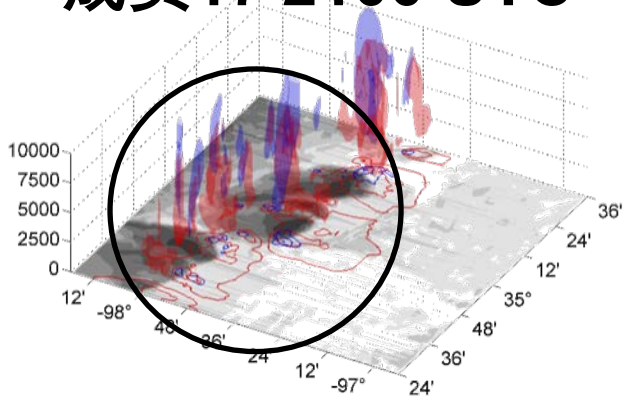
成员13 2140 UTC



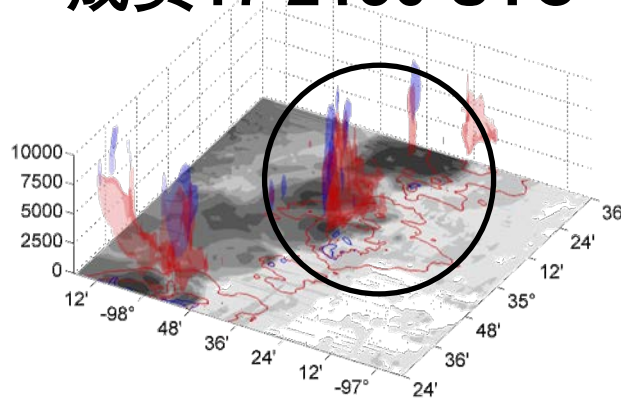
成员13 2200 UTC



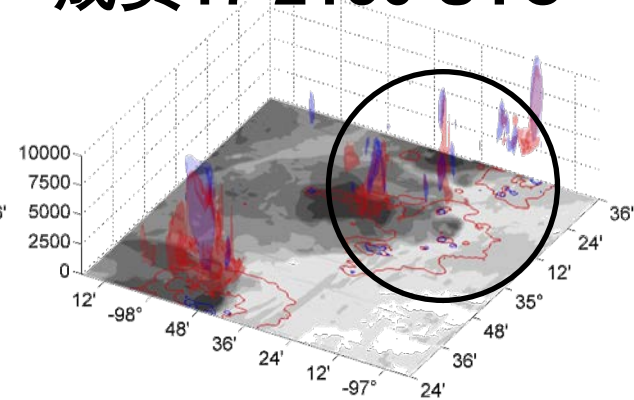
成员17 2100 UTC



成员17 2130 UTC



成员17 2150 UTC



60 dBZ 反射率  
20 m/s 垂直速度

两个雷暴再合并前的相互位置会影响合并之后新雷暴的发展和维持



# 总结

- 2013年5月20日发生在美国俄克拉荷马州的强对流雷暴天气过程的可预报性与尺度有关
  - 准线性对流系统的时间范围的可预报性较强，而单体雷暴的位置、强度和结构的可预报性有限（3~6小时）
  - 初始条件中天气条件和下垫面地形的误差导致水汽、不稳定性、垂直层结等对流条件和平均风场、风切变、低层辐合等动力条件的变化，影响对流的触发和组织
  - 湿对流过程和冷池与环境的相互作用会将微小的初始误差迅速放大并升尺度增长，使得预报技巧在初始误差减小90%的情况下依旧没有显著提高

- 对于数值预报实践的意义

- 如果对于天气背景的预报发生了时间的误差，以此为基础的模拟对流触发预报要相应地调整触发时间
- 当模拟对流触发出现位置误差时，简单地将模式模拟的雷暴过程进行平移并不能弥补预报误差
- 虽然强对流雷暴的本性可预报性极为有限，但是可以使用集合预报的方法，弥补初始场的不确定性
- 提供了强对流雷暴预报可能的误差量级

# 集合预报

## 本性可预报性

- 最理想条件下的可能 预报时效
- 有近乎完美的数值模式和初始条件

## 实际可预报性

- 当前技术条件下的最 长预报水平
- 受限于数值模式和初始条件中的误差

各种误差难以避免，决定了单一模式预报的局限，需要做考虑各种不确定性的集合预报。



# 集合预报： 爬线

# 问题：如何提高飓线的预报技巧？

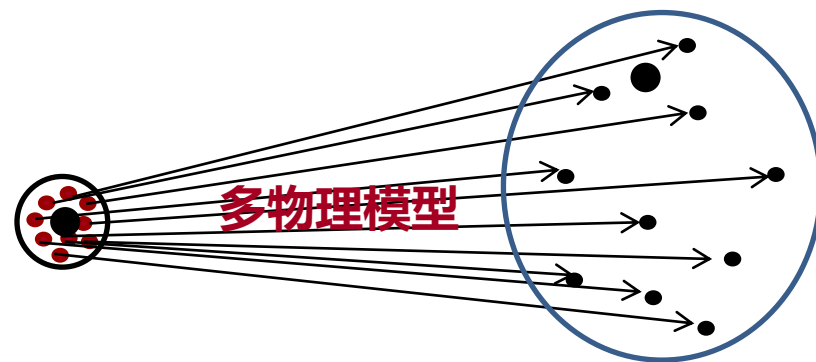
## 前人的工作：

大多仅考虑了初始场的不确定性，物理过程采用单一模型



## 我们的工作：

考虑物理过程的不确定性



(Wu, Meng, Yan, AAS, 2013)

# Impact of using a multi-scheme on the predictability

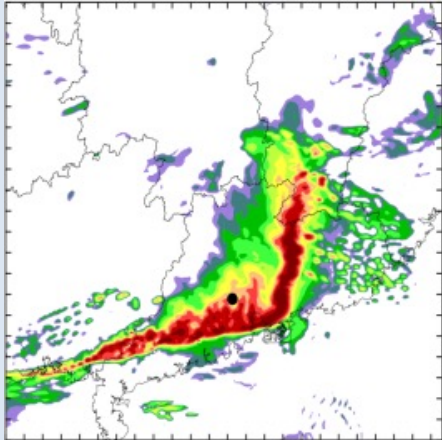
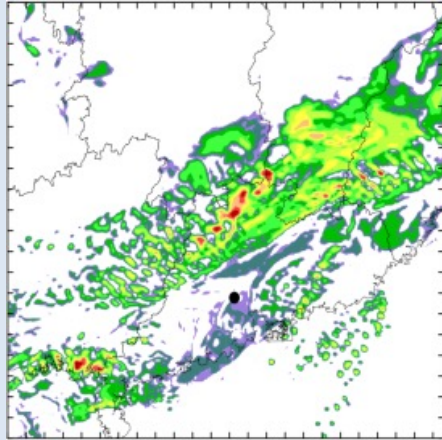
## Model configuration of Multi-scheme

No. of members using a cumulus scheme and the scheme used	No. of members using a microphysics scheme and the scheme used	No. of members using the PBL scheme and the scheme used	No. of members using the <u>longwave</u> scheme and the scheme used
13, <u>Kain-Fritsch</u>	4, Lin et al.	1,YSU;2,ETA;1,MRF	3,rrtm;1,cam
	4, Thompson et al.	1,YSU;2,ETA;1,MRF	3,rrtm;1,cam
	5, <u>WSM six-class graupel</u>	2,YSU;2,ETA;1,MRF	3,rrtm;2,cam
13, Betts-Miller	4, Lin et al.	1,YSU;2,ETA;1,MRF	3,rrtm;1,cam
	4, Thompson et al.	1,YSU;2,ETA;1,MRF	3,rrtm;1,cam
	5, WSM six-class <u>graupel</u>	2,YSU;2,ETA;1,MRF	3,rrtm;2,cam
14, <u>Grell-Devenyi</u>	4, Lin et al.	1,YSU;2,ETA;1,MRF	3,rrtm;1,cam
	5, Thompson et al.	2,YSU;2,ETA;1,MRF	3,rrtm;2,cam
	5, WSM six-class <u>graupel</u>	2,YSU;2,ETA;1,MRF	3,rrtm;2,cam

(Wu, Meng, Yan , AAS, 2012)

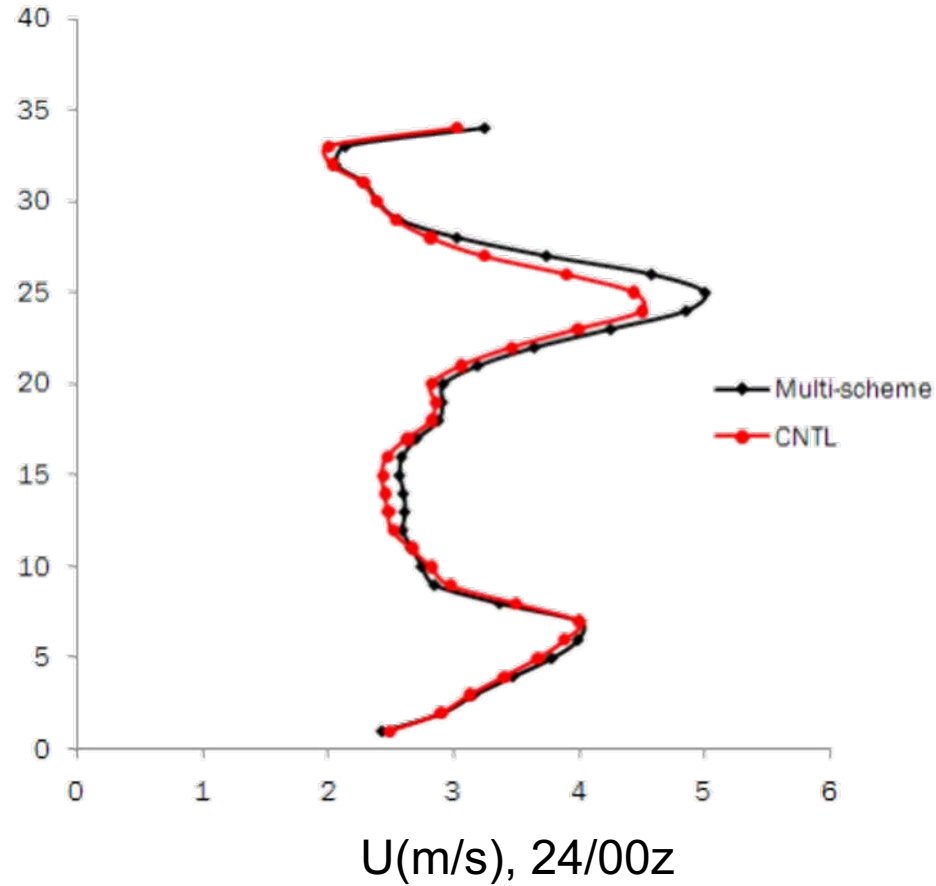


# 飊线的可预报性

	预报出飊线	没报出飊线
		
单物理模型	75%	25%
多物理模型	85%	15%

(Wu, Meng, Yan, AAS, 2013)

# Ensemble spread of **Multi** vs. **Single**



# Summary

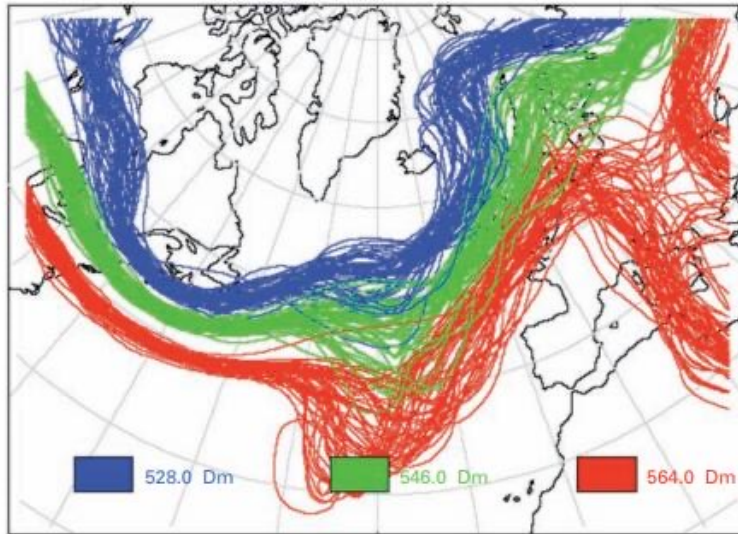
- **Model error apparently affect the predictability of the squall line**
  - Physical parameterization
  - Grid size
  - Cumulus parameterization
- **Initial error apparently affect the predictability of the squall line**
  - Linear impact
  - The moisture condition and moist processes played an important role
- **Adding physical perturbation helped to improve the forecast skill**



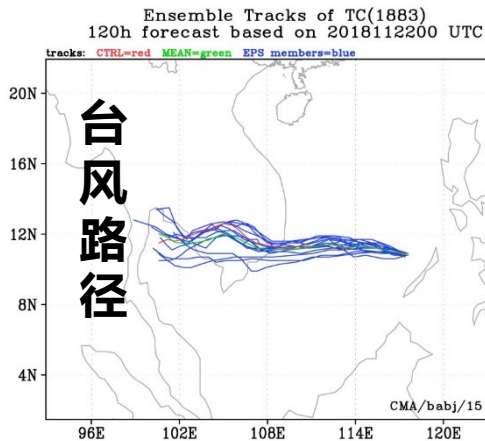
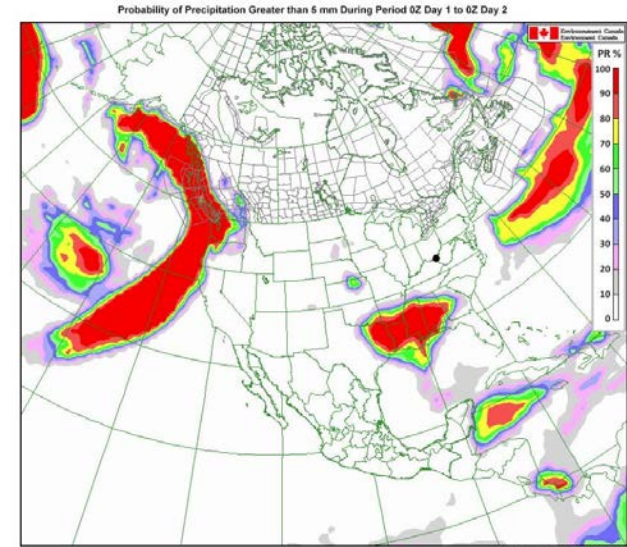
# 集合预报：台风

# 集合预报：平均场+可信度+发生概率

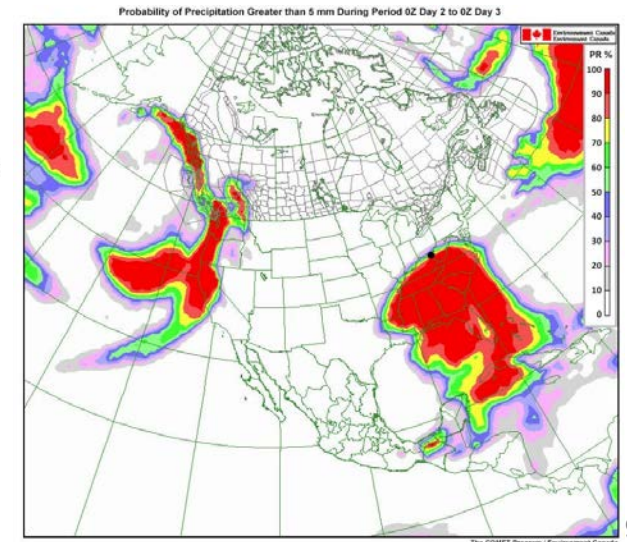
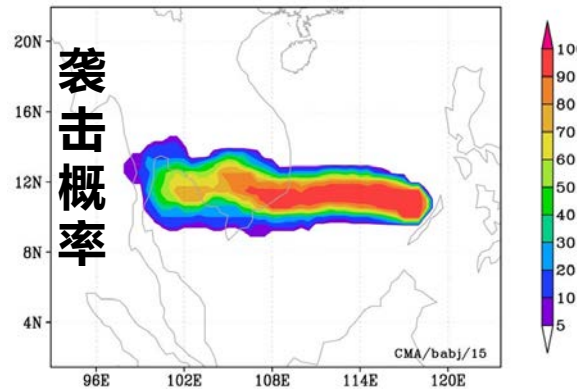
面条图



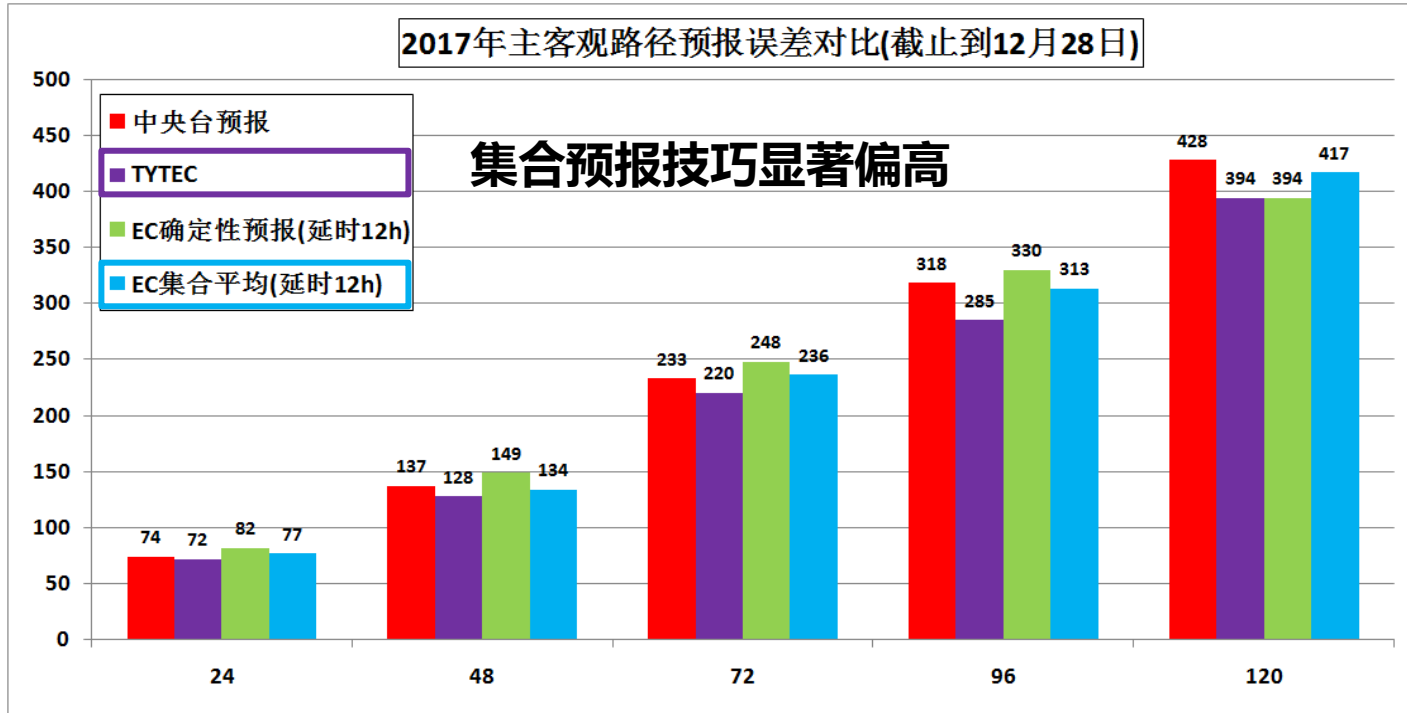
降水概率



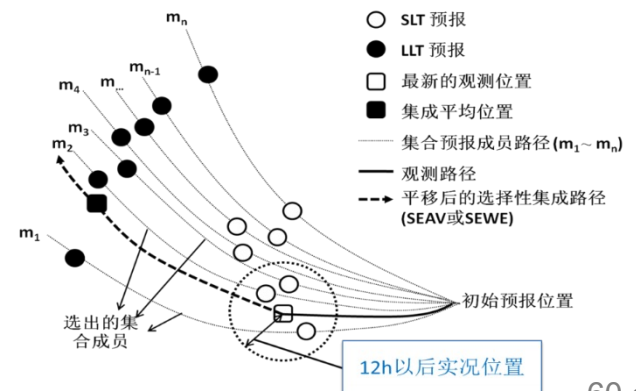
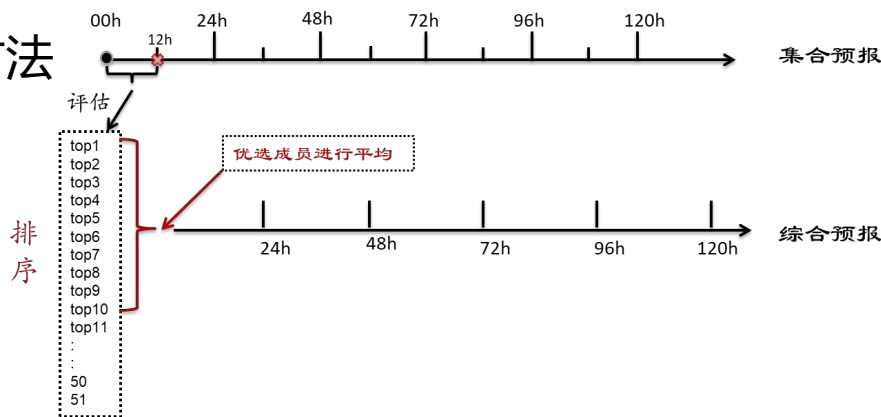
Probability that TC(1883) will pass within 120km radius  
During 120h forecast based on 2018112200 UTC



# 2017年台风路径预报技巧评估

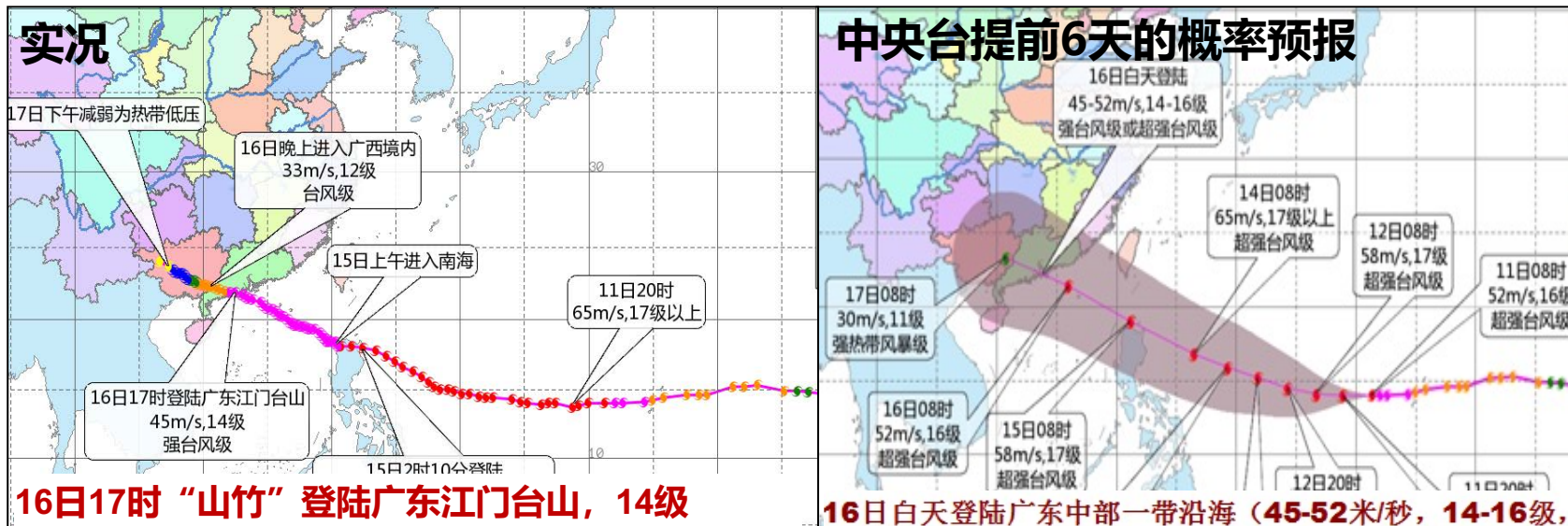


## TYTEC方法



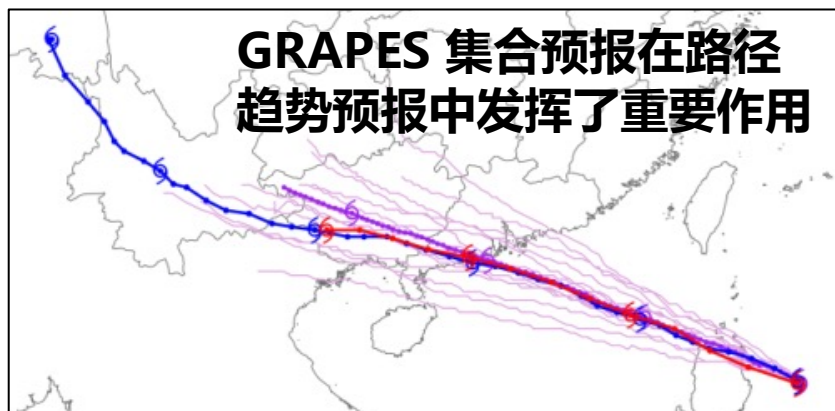


# 台风“山竹”的GRAPES 集合预报



GRAPES Track Forecasts for MANGKHUT (1822) Initialized at 2018091412 UTC

- GRAPES\_GFS (fcst=120h, inv=6h)
- GRAPES\_TYM (fcst=120h, inv=3h)
- MEPS\_members (fcst=84h, inv=1h)
- MEPS\_mean (fcst=84h, inv=1h)



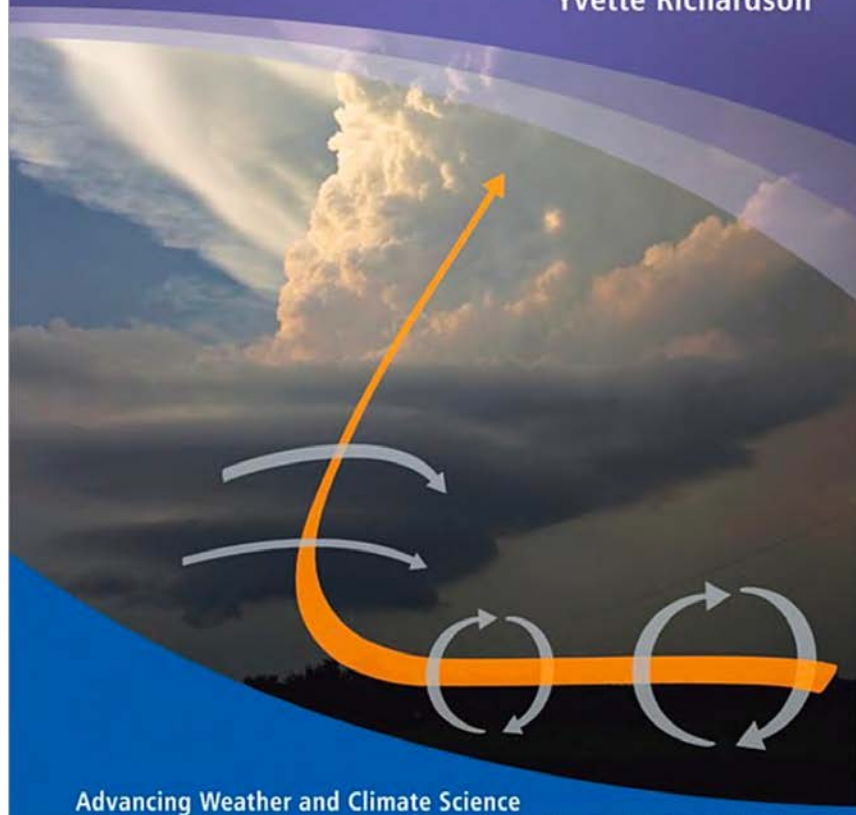
# 本课程期末回顾

WILEY-BLACKWELL

RMetS  
Royal Meteorological Society

# Mesoscale Meteorology in Midlatitudes

Paul Markowski  
Yvette Richardson



Advancing Weather and Climate Science

# Cloud Dynamics

Second Edition

Robert A. Houze, Jr.

AP INTERNATIONAL GEOPHYSICS SERIES, VOLUME 104



# Contents

Series Foreword	xi
Preface	xiii
Acknowledgments	xv
List of Symbols	xvii
<b>PART I General Principles</b>	<b>1</b>
<b>1 What is the Mesoscale?</b>	<b>3</b>
1.1 Space and time scales	3
1.2 Dynamical distinctions between the mesoscale and synoptic scale	5
<b>2 Basic Equations and Tools</b>	<b>11</b>
2.1 Thermodynamics	11
2.2 Mass conservation	16
2.3 Momentum equations	17
2.4 Vorticity and circulation	21
2.5 Pressure perturbations	25
2.6 Thermodynamic diagrams	32
2.7 Hodographs	34
<b>3 Mesoscale Instabilities</b>	<b>41</b>
3.1 Static instability	41
3.2 Centrifugal instability	48
3.3 Inertial instability	49
3.4 Symmetric instability	53
3.5 Shear instability	58
<b>PART II Lower Tropospheric Mesoscale Phenomena</b>	<b>71</b>
<b>4 The Boundary Layer</b>	<b>73</b>
4.1 The nature of turbulent fluxes	73
4.2 Surface energy budget	82
4.3 Structure and evolution of the boundary layer	83
4.4 Boundary layer convection	88

viii	CONTENTS	
4.5	Lake-effect convection	93
4.6	Urban boundary layers	103
4.7	The nocturnal low-level wind maximum	105
<b>5</b>	<b>Air Mass Boundaries</b>	<b>115</b>
5.1	Synoptic fronts	117
5.2	Drylines	132
5.3	Outflow boundaries	140
5.4	Mesoscale boundaries originating from differential surface heating	149
<b>6</b>	<b>Mesoscale Gravity Waves</b>	<b>161</b>
6.1	Basic wave conventions	161
6.2	Internal gravity wave dynamics	165
6.3	Wave reflection	170
6.4	Critical levels	172
6.5	Structure and environments of ducted mesoscale gravity waves	173
6.6	Bores	175
<b>PART III Deep Moist Convection</b>	<b>181</b>	
<b>7 Convection Initiation</b>	<b>183</b>	
7.1	Requisites for convection initiation and the role of larger scales	183
7.2	Mesoscale complexities of convection initiation	189
7.3	Moisture convergence	195
7.4	Elevated convection	197
<b>8 Organization of Isolated Convection</b>	<b>201</b>	
8.1	Role of vertical wind shear	201
8.2	Single-cell convection	206
8.3	Multicellular convection	209
8.4	Supercellular convection	213
<b>9 Mesoscale Convective Systems</b>	<b>245</b>	
9.1	General characteristics	245
9.2	Squall line structure	249
9.3	Squall line maintenance	253
9.4	Rear inflow and bow echoes	260
9.5	Mesoscale convective complexes	265

	CONTENTS	ix
<b>10 Hazards Associated with Deep Moist Convection</b>	<b>273</b>	
10.1	Tornadoes	273
10.2	Nontornadoic, damaging straight-line winds	292
10.3	Hailstorms	306
10.4	Flash floods	309
<b>PART IV Orographic Mesoscale Phenomena</b>	<b>315</b>	
<b>11 Thermally Forced Winds in Mountainous Terrain</b>	<b>317</b>	
11.1	Slope winds	317
11.2	Valley winds	320
<b>12 Mountain Waves and Downslope Windstorms</b>	<b>327</b>	
12.1	Internal gravity waves forced by two-dimensional terrain	327
12.2	Gravity waves forced by isolated peaks	332
12.3	Downslope windstorms	333
12.4	Rotors	342
<b>13 Blocking of the Wind by Terrain</b>	<b>343</b>	
13.1	Factors that govern whether air flows over or around a terrain obstacle	343
13.2	Orographically trapped cold-air surges	346
13.3	Lee vortices	351
13.4	Gap flows	358
<b>PART V Appendix</b>	<b>367</b>	
<b>A Radar and Its Applications</b>	<b>369</b>	
A.1	Radar basics	369
A.2	Doppler radar principles	371
A.3	Applications	374
<b>References</b>	<b>389</b>	
<b>Index</b>	<b>399</b>	

**Contents**

Dedication	v	2.5. Potential Vorticity	31
Preface	xiii	2.6. Perturbation Forms of the Equations of State and Continuity Equation	32
List of Symbols	xiv	2.6.1. Average and Linearization of the Thermodynamic and Water-Continuity Equations	32
		2.6.2. Flux Form and Linearization of the Thermodynamic and Water-Continuity Equations	32
		2.6.3. Flux Form and Linearization of the Equation of Motion	33
		2.6.4. Eddy Kinetic Energy Equation	33
		2.7. Oscillations and Waves	33
		2.7.1. Buoyancy Oscillations	33
		2.7.2. Gravity Waves	34
		2.7.3. Internal Oscillations	35
		2.7.4. Inertio-Gravitational Waves	36
		2.8. Adjustment to Geostrophic and Gradient Balance	36
		2.9. Instabilities	38
		2.9.1. Buoyant, Isentropic, and Symmetric Instabilities	38
		2.9.2. Kelvin-Helmholtz Instability	40
		2.9.3. Rayleigh-Brillouin Instability	42
		2.10. Representation of Eddy Fluxes	44
		2.10.1. k Theory	44
		2.10.2. Higher Order Closure	45
		2.10.3. Large Eddy Simulation	45
		2.11. The Planetary Boundary Layer	45
		2.11.1. The Urban Layer	46
		2.11.2. Boundary-Layer Stability	46
		2.11.3. The Surface Layer	46
		3. Cloud Microphysics	47
		3.1. Microphysics of Warm Clouds	47
		3.1.1. Nucleation of Droplets	47
		3.1.2. Condensation and Evaporation	49
		3.1.3. Fallspeeds of Drops	50
		3.1.4. Continuous Collection	51
		3.1.5. Stochastic Collection	52
		3.1.6. Spontaneous and Collisional Breakup of Drops and Modification of the Stochastic Collection Formulation	53
		3.2. Microphysics of Cold Clouds	54
		3.2.1. Homogeneous Nucleation of Ice Particles	54
		3.2.2. Heterogeneous Nucleation and Other Processes Forming Small Ice Particles in Clouds	55
		3.2.3. Vapor Deposition and Sublimation	58
		3.2.4. Aggregation and Riming	60
		3.2.5. Hail	61
		3.2.6. Ice Enhancement	62
		3.2.7. Fallspeeds of Ice Particles	62
		3.2.8. Melting	64
		3.3. Types of Microphysical Processes and Categories of Water Substance in Clouds	65
		3.4. Water-Continuity Equations	68
		3.4.1. General	68
		3.4.2. Bin Modeling of Warm Clouds	69
		3.4.3. Bin Modeling of Cold Clouds	70
		3.4.4. The Classic Kessler Approach to Bulk Water-Continuity Modeling of Warm Clouds	70
		3.4.5. Bulk Modeling of Cold Clouds by Extending the Kessler Scheme	74
		3.7. Water-Continuity Modeling of Cold Clouds Using Generalized Mass-Scale and Area-Scale Relations	75
		4. Remote Sensing of Clouds and Precipitation	77
		4.1. Absorption, Scattering, and the Microwave Domain	78
		4.2. Passive Microwave Sensing of Precipitation	79
		4.3. Radar Sensing of Clouds and Precipitation	80
		4.4. Radar Reflectivity from Returned Power	82
		4.5. Radar Polarimetry	84
		4.5.1. Parameters Measured by Dual-Polarization Radar	84
		4.5.2. Identification of Hydrometeor Type with Dual-Polarization Radar	85
		4.6. Relating Radar Measurements to Hydrometeor Concentration, Precipitation, Fall Velocity, and Cloud-System Structure	86
		4.6.1. Particle-Size Method	87
		4.6.2. Rain-Gauge Method	87
		4.6.3. Polarimetric Improvement of Rain Estimation	88
		4.7. Estimating Areal Precipitation from Radar Data	88
		4.8. Determining Cloud Morphology from Radar Data	89
		4.9. Doppler Radar	91
		4.9.1. Radial Velocity	91
		4.9.2. Velocity and Range Folding	91
		4.9.3. Vertical Incidence Observations	91
		4.9.4. Range-Height Data	92
		4.9.5. Velocity-Azimuth Display Method	92
		4.9.6. Multiple Display Synthesis	94
		4.9.7. Retrieval of Thermodynamic and Microphysical Variables	95

**Part II**

**Phenomena**

5. Clouds in Shallow Layers at Low, Middle, and High Levels	101
5.1. Fog and Stratus Occurring in a Boundary Layer Cooled from Below	101
5.1.1. General Considerations	101
5.1.2. Radiation Mixing in Fog	102
5.1.3. Turbulent Fog	104
5.1.4. Arctic Stratus and Stratocumulus	108
5.2. Stratocumulus Forming in Boundary Layers Heated from Below	111
5.2.1. Conceptual Model of the Formation of a Cloud Topped Mixed Layer	112
5.2.2. Mathematical Modeling of Cloud Topped Mixed Layer Formation	112
5.2.3. Stratocumulus with Drizzle	118
5.2.4. Later Stages of the Stratocumulus Lifecycle	118
5.2.6. Cellular Structures and Patterns in Stratocumulus Fields	118
5.2.7. Boundary Layer Rolls and Cloud Streets	120
5.3. Alrostratus and Altostratus	124
5.3.1. Alrostratus and Altostratus Produced as Remnants of Other Clouds	124
5.3.2. Altostratus as High Based Convective Clouds	125
5.3.3. Alrostratus and Altostratus in Shallow Layer Clouds Aloft	125
5.3.4. Ice Particle Generation by Altostratus Elements	127
5.3.5. Interaction of Altostratus and Lower Cloud Layers	127

5.4. Cirriform Clouds	127
5.4.1. Nomenclature	127
5.4.2. Climatology and Origins of Cirriform Clouds	128
5.4.3. Microphysics, Vertical Air Motions, and Radiation from Cirriform Clouds	130
5.4.4. Small Cirriform Convective Elements—“Generating Cells”	132
5.4.5. Buoyant Anvil Dynamics	133
5.4.6. Radiative Destabilization and Shear Effects on a Layer of Cirriform Cloud	137
5.4.7. Mesoscale Circulation Induced by Radiative Heating of a Layer of Cirriform Cloud	138
6. Nimbostratus and the Separation of Convective and Stratiform Precipitation	141
6.1. Definition of Stratiform Precipitation and How It Differs from Convective Precipitation	142
6.2. The Contrasting Radar-Echo Structures of Stratiform and Convective Precipitation	144
6.3. Microphysical Observations in Nimbostratus and Implied Vertical Air Motions	146
6.4. Role of Convection in Regions of Stratiform Precipitation	147
6.5. Stratiform Precipitation with Shallow Overlying Convective Cells Aloft	147
6.6. Stratiform Precipitation Produced by Deep Convection	152
6.6.1. Particle Fronts and the Evolution of Deep Convective Cells into Nimbostratus	152
6.6.2. Stratiform Precipitation Produced by Discrete Redevlopment of Deep Convection	154
6.6.3. Stratiform Precipitation Produced by Convective Redevlopment in a Variable Wind Shear Environment	156
6.6.4. Microphysics of the Stratiform Precipitation Associated with Deep Convective Systems	157
6.7. Radiative Effects on Nimbostratus	163
6.8. Separation of Convective and Stratiform Precipitation	162
7. Basic Cumulus Dynamics	165
7.1. Buoyancy	165
7.2. The Pressure Perturbation Field Associated with Buoyancy	166
7.3. Entrainment and Detrainment	167
7.3.1. General Consideration	167
7.3.2. Early Views of Mixing with the Cloud's Environment	168
7.3.3. More Realistic Views of Entrainment and Detrainment	175
7.3.4. Effect of Entrainment on Buoyancy and Downward Motion Near Cloud Edge	176
7.3.5. Lateral Versus Cloud-Top Entrainment	176
7.3.6. Convective Cloud in a Fixed Column	177
7.3.7. Representation of Mixing in Multidimensional Models of Convective Clouds	180
7.3.8. Representation of Convective Clouds in Large Scale Models of the Atmosphere	182
7.4. Vorticity and Dynamic Pressure Perturbation Forces	181
7.4.1. The Vorticity Approach to Understanding Rotation and Dynamic Pressure in Convective Clouds	182
7.4.2. Horizontal Vorticity	182
7.4.3. Vertical Vorticity Introduced by Tilting of Environment Horizontal Vorticity	183
7.4.4. Effects of Vortices on Entrainment and Pressure Perturbation	183
8. Cumulonimbus and Severe Storms	187
8.1. The Basic Cumulonimbus Cloud	187
8.2. Multicell Storms	194
8.3. Supercell Storms	194
8.4. Environmental Conditions Favoring Different Types of Deep Convective Storms	198
8.5. Supercell Dynamics	201
8.5.1. Storm Splitting and Propagation	203
8.5.2. Directional Shear in the Environment of the Cumulonimbus Cloud	204
8.5.3. Updraft Rotation	205
8.5.4. Helicity and the Strength of Supercell Updraft Rotation	207
8.5.5. Baroclinity Associated with Downdrafts	207
8.5.6. The Three Sources of Rotation in a Supercell	207

8.6. Tomadogenesis in Supercell Storms	208
8.6.1. The Primary Factors Contributing to Tomadogenesis in a Supercell	208
8.6.2. Occlusion Downdrafts, the Surface Mesocyclone, and Vortex Breakdown	209
8.7. Ground Tracks of Supercell Storms	210
8.8. Non-Supercell Thunderstorms and Waterspouts	211
8.9. The Tornado	211
8.9.1. Observed Structure and Life Cycle of a Tornado	213
8.9.2. Vortex Dynamics	215
8.9.3. Vortex Breakdown	219
8.9.4. Multiple Vortex Tornadoes	221
8.10. Downbursts and Microbursts	221
8.10.1. Definitions and Descriptive Models	222
8.10.2. Effects of Microbursts on Aircraft	223
8.10.3. Mechanisms Driving Microbursts	224
8.10.4. Downburst Rotor Circulations and Outflow Winds	227
8.11. Gull Fronts, Derechos, and Area Clouds	227
8.11.1. Gull Front Phenomena and Nonvorticity	227
8.11.2. Gravity Current Dynamics	228
8.12. Lines of Convective Storms	231
9. Mesoscale Convective Systems	237
9.1. General Characteristics	237
9.1.1. Satellite Observed Cloud Tops and the Most Intense MCSs	237
9.1.2. Precipitation and a More General Definition of an MCS	238
9.1.3. Sizes of MCSs	240
9.1.4. Basic Components of an MCS	241
9.1.5. Internal Structure	241
9.1.6. Life Cycle	243
9.2. Leading-Edge-Trailing-Stratiform Structure	245
9.2.1. Radar Echo Structure and Vertical Air Motions	245
9.2.2. Microphysical Structure	247
9.2.3. Forward Outflowing Rear Inflow, and Ascending Feet to Rear Flow	248
9.2.4. Precipitation Processes and Trajectories	248
9.2.5. Pressure Pattern	248
9.2.6. Electrical Structure	249
9.3. Bulk Dynamical View	250
9.3.1. Layered Mesoscale Anvil	250
9.3.2. Simulations of Two-Dimensional Steady State Anvil and Descend	250
9.3.3. Wave Interpretations	254
9.3.4. The Crossover Zone	256

9.4. Details of the Convective Region	258
9.4.1. Observed Anvil	258
9.4.2. Pressure-Perturbation Field	259
9.4.3. Thermal and Water-Vapor Perturbations	261
9.4.4. Multicellular Aspect of the Convective Line and Cell Life Cycle	262
9.4.5. Gravity Waves and Interaction with the Stratopause	265
9.4.6. Bow Echo Formation and Effects of the Stratiform Region on the Convective Region	266
9.5. Details of the Stratiform Region	268
9.5.1. Updraft Air Motion and Precipitation Development in the Stratiform Cloud	268
9.5.2. Thermodynamic Structure of the Stratiform Region	272
9.5.3. The Mesoscale Downdraft	274
9.5.4. Kinematic and Thermodynamic Structure at the Top of the Stratiform Cloud	275
9.5.5. The Wake Low	277
9.5.6. Midlevel Inflow to the Mesoscale Downdraft	277
9.6. Divergence, Duality Processes, and Vorticity	281
9.6.1. The Divergence Profile	281
9.6.2. The Distribution of Heating and Cooling	282
9.6.3. Vortex Development	282
10. Clouds and Precipitation in Tropical Cyclones	287
10.1. Definitions, Climatology, and the Synoptic-Scale Contexts of Tropical Cyclones	287
10.2. Clouds Involved in Tropical Cyclogenesis	288
10.2.1. Idealization of the Clouds in an Intensity Depression	288
10.2.2. Example of a Vertical Hot Tower	290
10.2.3. Ensemble of Clouds in a Developing Storm	290
10.2.4. Cloud Feedback in Cyclogenesis	290
10.3. Overview of the Mature Tropical Cyclone	293
10.3.1. Visible Clouds	293
10.3.2. Three-Dimensional Wind Field	293
10.3.3. Steady State Anvil and Descend and Angular Momentum in Relation to the Eye and Eyewall	295

10.4. The Eye	296
10.5. Dynamics of the Mean Eyewall Cloud	299
10.5.1. Sloping Angular Momentum Surfaces	299
10.5.2. Boundary Layer Assumptions and Implications	300
10.5.3. Connecting the Balanced Vortex with a Simplified Boundary Layer	301
10.5.4. Thermodynamic Relationships Applied in the Eyewall Region	302
10.5.5. Characteristics of the $\beta$ Surfaces Above the Boundary Layer	302
10.5.6. Relating $\beta$ and $R_e$ Surfaces in the Boundary Layer	302
10.5.7. Properties of the Top of Boundary Layer in the Eyewall Region	303
10.5.8. Solutions for the $\beta$ and $R_e$ Surfaces in the Eyewall Cloud	304
10.5.9. Temporal Development and Stability of the Mean Two-Dimensional Eyewall Cloud	305
10.6. Substructure and Asymmetry of the Eyewall Cloud	306
10.6.1. Conditional Instability Within the Eyewall Cloud	306
10.6.2. Eyewall Vorticity Anisotropy and Strong Updrafts	308
10.6.3. Outflows and Precipitation	309
10.6.4. Downbursts in the Eyewall	311
10.6.5. Vertical Asymmetry Owing to Storm Motion and Shear	312
10.6.6. Cloud Microphysical Processes in the Eyewall and Inner Core Region	313
10.6.7. Electric Fields of the Eyewall	315
10.7. The Region Beyond the Eyewall: Rainbands and Eyewall Replacement Complex—An Overview	315
10.7.1. The Eyewall/Rainband Complex—An Overview	319
10.7.2. The Principal Rainband	319
10.7.3. The Principal Rainband	319
10.7.4. Vortex Rossby Waves and Secondary Rainbands	322
10.7.5. Eyewall Contraction and Replacement	325

11.1.1. Idealized Horizontal and Vertical Structure	330
11.1.2. Dynamics Governing Large Scale Vertical Air Motion	331
11.1.3. Application of the Omega Equation to a Real Baroclinic Wave	333
11.1.4. Low-Level Cyclone Development	334
11.1.5. Development of the Thermal Pattern in the Eyewall Region	334
11.2. Circulation at a Front	334
11.2.1. Quasigeostrophic Frontogenesis	335
11.2.2. Semigeostrophic Frontogenesis	337
11.2.3. Moist Frontogenesis	340
11.2.4. Some Simple Theoretical Examples	341
11.3. Horizontal Patterns of frontal Zones and Developing Cyclones	344
11.4. Clouds and Precipitation in a frontal Cyclone	347
11.4.1. Water-Vapor Influx, Atmospheric Rivers, and the Warm Conveyor Belt	347
11.4.2. Satellite Observed Cloud Patterns	347
11.4.3. Distribution of Precipitation Within the Cloud Pattern	349
11.4.4. Warm Cold Frontal Rainbands	352
11.4.5. Wide Cold Frontal Rainbands	355
11.4.6. Warm Frontal Rainbands	357
11.4.7. Clouds and Precipitation Associated with the Frontage of Warm Air Aloft	361
11.4.8. Rainbands in the Corona Head of the Cyclone	362
11.5. Clouds in Polar Lows	363
11.5.1. Coronal Cloud Systems	363
11.5.2. Tropical Cyclone Dynamics in Cold Airinflow	365
12. Clouds and Precipitation Associated with Hills and Mountains	369
12.1. Shallow Clouds in Stable Upflow Flow	370
12.2. Wave Clouds Produced by Long Ridges	370
12.2.1. Flow over Sinusoidal Terrain	370
12.2.2. Flow over a Ridge of Arbitrary Shape	372
12.2.3. Clouds Associated with Vertically Propagating Waves	373
12.2.4. Clouds Associated with Low Waves	374
12.2.5. Nonlinear Effects: Large Amplitude Waves, Blocking the Hydraulic Jump, and Rotor Clouds	376

关于本课程，你有什么建议？